AFRL-IF-RS-TR-2004-76
Final Technical Report
March 2004

MECHANICAL PROPERTIES OF MEMS MATERIALS

Johns Hopkins University

Sponsored by
Defense Advanced Research Projects Agency
DARPA Order No. J346

APPROVED FOR PUBLIC RELEASE; DISTRIBUTION UNLIMITED.

The views and conclusions contained in this document are those of the authors and should not be interpreted as necessarily representing the official policies, either expressed or implied, of the Defense Advanced Research Projects Agency or the U.S. Government.

AIR FORCE RESEARCH LABORATORY
INFORMATION DIRECTORATE
ROME RESEARCH SITE
ROME, NEW YORK

STINFO FINAL REPORT

This report has been reviewed by the Air Force Research Laboratory, Information Directorate, Public Affairs Office (IFOIPA) and is releasable to the National Technical Information Service (NTIS). At NTIS it will be releasable to the general public, including foreign nations.

AFRL-IF-RS-TR-2004-76 has been reviewed and is approved for publication.

APPROVED: /s/
CLARE D. THIEM
Project Engineer

FOR THE DIRECTOR: /s/
JAMES A. COLLINS, Acting Chief
Information Technology Division
Information Directorate

REPORT DOCUMENTATION PAGE

Form Approved
OMB No. 074-0188

Public reporting burden for this collection of information is estimated to average 1 hour per response, including the time for reviewing instructions, searching existing data sources, gathering and maintaining the data needed, and completing and reviewing this collection of information. Send comments regarding this burden estimate or any other aspect of this collection of information, including suggestions for reducing this burden to Washington Headquarters Services, Directorate for Information Operations and Reports, 1215 Jefferson Davis Highway, Suite 1204, Arlington, VA 22202-4302, and to the Office of Management and Budget, Paperwork Reduction Project (0704-0188), Washington, DC 20503

1. AGENCY USE ONLY (Leave blank)	2. REPORT DATE	3. REPORT TYPE AND DATES COVERED
	MARCH 2004	**FINAL** Oct 99 – Sep 02

4. TITLE AND SUBTITLE

MECHANICAL PROPERTIES OF MEMS MATERIALS

5. FUNDING NUMBERS

C - F30602-99-2-0553
PE - 63739E
PR - E117
TA - 00
WU - 50

6. AUTHOR(S)

W. N. Sharpe, Jr., K. J. Hemker - Dept of Mechanical Engineering
R. L. Edwards - Applied Physics Laboratory

7. PERFORMING ORGANIZATION NAME(S) AND ADDRESS(ES)

Department of Mechanical Engineering
Johns Hopkins University
Baltimore MD 21218

Applied Physics Laboratory
Johns Hopkins University
Laurel MD 20723

8. PERFORMING ORGANIZATION REPORT NUMBER

N/A

9. SPONSORING / MONITORING AGENCY NAME(S) AND ADDRESS(ES)

Defense Advanced Research Projects Agency
3701 North Fairfax Drive
Arlington VA 22203-1714

AFRL/IFTC
26 Electronic Parkway
Rome NY 13441-4514

10. SPONSORING / MONITORING AGENCY REPORT NUMBER

AFRL-IF-RS-TR-2004-76

11. SUPPLEMENTARY NOTES

AFRL Project Engineer: Clare D. Thiem/IFTC/(315) 330-4893 Clare.Thiem@rl.af.mil

12a. DISTRIBUTION / AVAILABILITY STATEMENT

APPROVED FOR PUBLIC RELEASE; DISTRIBUTION UNLIMITED.

12b. DISTRIBUTION CODE

13. ABSTRACT ***(Maximum 200 Words)***

New techniques and procedures were developed to measure the mechanical properties of the thin-film structural materials used in microelectromechanical systems. Tensile stress-strain curves were measured for polysilicon, silicon nitride, silicon carbide, and electroplated nickel. For example, polysilicon has a Young's modulus of 160 GPa and a Poisson's ratio of 0.22. It is a linear brittle material with fracture strength as high as 3 GPa. The mechanical properties of electroplated nickel are found to be highly dependent on the manufacturing process. Preliminary tests were conducted on silicon germanium, aluminum-glass composites, and diamond (amorphous carbon). Tests on specimens with stress concentrations show a definite size effect, i.e., increase in fracture strength with decrease in size of highly stressed region, that is explained with Weibull statistics.

Scanning and transmission electron microscopy studies of these materials relate the microstructure to the mechanical behavior. X-ray and atomic force microscopy studies show texture and surface roughness to be important features. Methods were developed to test polysilicon up to 600°C, and it is seen to be ductile and subject to creep at these temperatures. The coefficient of thermal expansion of polysilicon is larger than predicted from single crystal data. New axial fatigue tests at 6 kHz show polysilicon to behave much like a metal with decreased loading leading to increased life. Creep and fatigue tests were also conducted on nickel.

14. SUBJECT TERMS

MEMS, Young's modulus, Poisson's ratio, fracture strength, fatigue, creep, high temperature, polysilicon, nickel, silicon nitride

15. NUMBER OF PAGES 60

16. PRICE CODE

17. SECURITY CLASSIFICATION OF REPORT	18. SECURITY CLASSIFICATION OF THIS PAGE	19. SECURITY CLASSIFICATION OF ABSTRACT	20. LIMITATION OF ABSTRACT
UNCLASSIFIED	UNCLASSIFIED	UNCLASSIFIED	UL

NSN 7540-01-280-5500

Standard Form 298 (Rev. 2-89)
Prescribed by ANSI Std. Z39-18
298-102

TABLE OF CONTENTS

	Page
List of Figures	**iii**
List of Tables	**vi**
Foreword	**vii**
1.0 – Introduction	**1**
2.0 - Polysilicon stress-strain at temperature and CTE.	**1**
3.0 - Case Western silicon carbide.	**8**
4.0 - Other thin-film materials.	**9**
5.0 - Diamond stress-strain curves.	**15**
6.0 - Polysilicon fatigue.	**17**
7.0 - Polysilicon creep.	**20**
8.0 - Thin film microstructural studies.	**22**
9.0 - Modeling of thin films.	**26**
10.0 - LIGA nickel stress-strain at temperature and TCE.	**28**
11.0 - MIT silicon carbide.	**34**
12.0 - LIGA nickel fatigue.	**35**
13.0 - LIGA nickel Creep.	**37**
14.0 - Thick film microstructural studies.	**39**
15.0 - Modeling of thick films.	**40**
16.0 – Summary	**40**
17.0 - References	**41**

18.0 - Overview and Review Publications **42**

19.0 - Presentations **43**

20.0 - Personnel and Collaborators **45**

LIST OF FIGURES

Page

Figure 2.1 - Stress versus biaxial strain for polysilicon. 2

Figure 2.2 – Young's modulus and fracture strength for four materials. 3

Figure 2.3 – Comparison of strengths of Sandia polysilicon measured in three laboratories. 3

Figure 2.4 – Variation in Young's modulus with temperature for polysilicon. 4

Figure 2.5 – A 600 μm wide polysilicon specimen at 600°C. 5

Figure 2.6 – Polysilicon at 25°C and 670°C (left) and 700°C (right). 5

Figure 2.7 – Thermal strain for polysilicon. 6

Figure 2.8 – Schematic of the notched specimens. 7

Figure 2.9 – Predicted versus measured fracture stresses for a double-notched specimen 20 μm wide. 7

Figure 3.1 – A silicon carbide specimen from CWRU; it is 0.5 μm thick. 8

Figure 3.2 – Stress-strain curve for CWRU silicon carbide. 9

Figure 4.1 – A silicon nitride specimen. It is 0.5 μm thick and 600 μm wide. 10

Figure 4.2 – Stress versus biaxial strain for silicon nitride. 11

Figure 4.3 – A tensile and a bulge test specimen of silicon nitride. The die is one cm square in each case. 12

Figure 4.4 – A silicon germanium specimen on a die with other microdevices. 13

Figure 4.5 – Force versus displacement for a silicon germanium specimen. 13

Figure 4.6 – CMOS tensile specimens and thermal actuators on a die from Carnegie Mellon. 14

Figure 4.7 – Stress versus displacement for CMOS specimens with different layers. **15**

Figure 5.1 – Diamond specimens from Sandia. **16**

Figure 5.2 – A diamond tensile specimen with fiber attached. The test section is 1.5 μm thick, 20 μm wide, and 250 μm long. **16**

Figure 5.3 – Stress versus displacement for diamond. **17**

Figure 6.1 – Photograph of the fatigue test setup. **18**

Figure 6.2 – Stress versus number of cycles to failure for polysilicon **18**

Figure 6.3 – Static fatigue results for polysilicon in air and water. **19**

Figure 7.1 – Creep behavior of polysilicon at different temperatures and loads. **20**

Figure 7.2 – Photograph of a narrow creep specimen with a fiber glued to the grip end. **21**

Figure 7.3 – Creep results for a wide and a narrow specimen at 600°C and 0.4 GPa. **21**

Figure 8.1 - TEM micrographs of (a): Cronos (MUMPS 25) and (b): SMI Polysilicon Thin Films. **23**

Figure 8.2 - {111} and {110} contours level of the x-rayed Cronos sample showing that {110} planes are parallel to the film surface. **23**

Figure 8.3 - SEM micrograph of the fracture surface of a polysilicon **24**

Figure 8.4 - AFM profile of the top surface of a polysilicon sample. **24**

Figure 8.5 - TEM cross-sectional (left) and top view of the as-received SiC thin film. **25**

Figure 8.6 - Texture Evolution of SiC Thin film. 1: as received; 2: heat-treated @ 200°C-2h, showing the scattering of the <111> fiber. **26**

Figure 9.1 – Predicted and measured temperatures along the length of a wide specimen. **27**

Figure 9.2 – Effect of gold markers on measured strain. **28**

Figure 10.1 - Room temperature tensile tests of LIGA Ni samples that have been annealed for 1 hour at various temperatures. **29**

Figure 10.2 - Effect of test temperature on the properties of LIGA Ni structures. **31**

Figure 10.3 - Measurements of the CTE of LIGA Ni. **32**

Figure 10.4 - Force vs. Displacement curve for Spring 12 along with photographs of the deformed states. **33**

Figure 11.1 – A silicon carbide specimen from MIT; it is 30 μm thick. **34**

Figure 11.2 – Stress-strain curve for MIT silicon carbide. **35**

Figure 12.1 - Optical micrograph of ASTM standard E466 LIGA Ni fatigue specimens; width is 50 μm and specimens are 3.7 mm long. **36**

Figure 12.2 - LIGA Ni fatigue data. **37**

Figure 13.1 - Creep curves of LIGA Ni at relatively modest temperatures. **38**

Figure 13.2 - Composite plot of the temperature and stress dependence of creep rates measured in this study. **38**

Figure 14.1 - Cross-section optical micrographs of LIGA Ni specimens heat-treated to a variety of times and temperatures. **39**

Figure 14.2 - Comparison of cross-section SEM micrographs of the fracture surfaces of LIGA Ni specimens tested in fatigue and creep with the as-deposited grain structure. **40**

LIST OF TABLES

Page

Table 3.1 – Properties of CWRU silicon carbide. 9

Table 4.1 – Results from comparison tests. 12

Table 11.1 – Properties of MIT silicon carbide. 35

Foreword

New test methods were developed and new material properties measured in the course of this project. The effort was divided into 14 separate tasks (some much more extensive than others), which are summarized in some detail in the body of the report. Some comments of an overview nature are made first.

Specimens

Three kinds of specimens were tested – wide, narrow, large – each having particular advantages.

Wide Specimen – These are thin films deposited onto a one-centimeter square silicon die cut from a wafer. A rectangular window is etched into the substrate from the back to free the tensile gage section shown in the photograph below. After the two large ends are glued into a test machine, the side support strips are cut with a diamond saw. Reflective lines deposited in the center of the test section enable biaxial strain measurement.

Narrow Specimen – These thin films are deposited in groups of 14-18 onto a one-centimeter square die. The gage section shown below is 50 µm wide and 2 mm long. The right end remains fastened to the substrate and the rest of the specimen along with the large grip end at the left are freed by etching. After a fiber is glued to the grip, the four support straps are cut. The two reflective lines enable strain measurement.

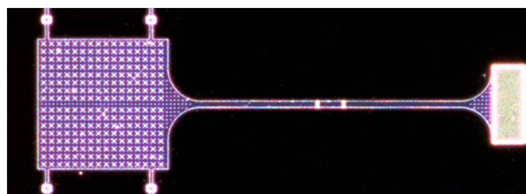

Large Specimen – The specimen pictured is 3.1 mm long with a gage section 200 µm by 200 µm. These thick-film (30–200 µm) specimens can be picked up with tweezers and placed into grip inserts that match the wedge-shaped ends. Strain is measured using reflective indentations.

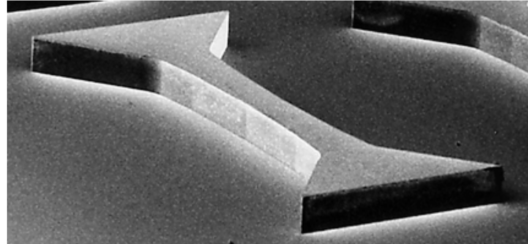

Strain Measurement

A key and unique feature of this research is the capability of measuring strain directly on tensile specimens. This approach, which is routinely used in macroscopic material testing, avoids the complications of indirect measurements where material properties are extracted from models of test structures. Further, it enables unambiguous determination of the entire stress-strain curve from which the properties are obtained.

The strain measurement technique is known as the ISDG (Interferometric Strain/Displacement Gage). Two reflective lines a few hundred microns apart are deposited onto the gage section of the specimen. When they are illuminated with a laser, interference fringes form in space. As the specimen is strained, the relative displacement of the lines causes movement of the fringes. This fringe movement is monitored with linear diode arrays and a laboratory computer to provide real-time strain measurement. When two pairs of lines are placed orthogonally, biaxial strain and Poisson's ratio can be measured.

New Mechanical Test Methods

Many valuable contributions to mechanical testing of MEMS materials were made in the course of this project, but some are truly exceptional:

- A test method for MEMS materials was established that is regarded by some as a 'gold standard'. The continued application and refinement of the techniques and procedures that had been initiated prior to the project built a basis for confidence within the community. The comparative tests on silicon nitride served to strengthen this view. The ASTM tensile test is the basic one for determining the material properties of structural materials, and it has been adapted to the microscale.
- The very first tensile tests on a number of thin-film materials were conducted. Test methods were developed for an extensive series of tests on silicon carbide from two different sources.

- The techniques developed for testing at high temperature set the stage for future studies of various materials. In particular, showing that polysilicon begins to deform plastically and to creep at temperatures above 500°C is especially important to designers of thermal actuators.
- The fatigue results for polysilicon are the most thorough and unambiguous in existence. Other test methods require finite element analyses of very complicated stress concentrations to determine the stress, but ours is simply force/area. The fact that polysilicon shows the same type of fatigue behavior as metals and is independent of frequency will be a major factor to be considered by designers.

‘Handbook’ Data

Some materials have been tested in sufficient numbers that the results may be regarded as ‘handbook’ values, i.e. they may be used in initial designs. Such results are actually the ultimate goal of experimental research of this nature. The table below lists them, and it should be noted that this is the first such listing for materials that were all tested in the same laboratory.

	Specimen shape	**Young’s modulus (GPa)**	**Strength (GPa)**
Polysilicon	Wide and Narrow	158	1.2 – 3.0
Silicon Nitride	Wide	254	6.4
Thin Silicon Carbide	Wide	420	1.2
Thick Silicon carbide	Wide	430	0.5
Silicon Germanium	Narrow	--	1.0
Diamond	Narrow	--	3.8
LIGA Nickel	Large	165-210 (depends on texture)	0.36 - 0.90 (depends on current)

General Comments

This was a multi-faceted research project involving new experimental methods, new materials, and several organizations. In contrast to a more traditional research program in which one uses well-established approaches (e. g. macroscale tensile testing and Transmission Electron Microscopy) to study novel materials produced in-house, almost everything had to be developed during the course of the project. It may be useful to make some general observations.

- There were some deviations from the original plan as would be expected in any research program – particularly one involving such a new technology. The major one was the renaming of a task from 'PZT stress-strain curves' to 'Other thin-film materials'. This occurred because the Army Research Laboratory had difficulty in making PZT specimens. As word of the work spread, specimens of other materials such as silicon nitride, CMOS composites, silicon germanium, and amorphous silicon were provided by collaborators.

- Additions were made to the original plan in that new research was undertaken as opportunities arose. The premier example here is the testing of notched polysilicon specimens. As the test methods for polysilicon matured, it became evident that studying the effect of stress concentrations on the strength of this brittle material would be important. A thorough study, in cooperation with NASA Glenn personnel, was conducted and may well be one of the most important contributions.

- It is difficult to rely on other research organizations to supply specimens. In some cases, such as silicon carbide, the deposition process itself was undergoing development and early specimens were not usable. In other cases, the promised specimens were simply never provided. It is also difficult to rely on other organizations for certain tasks. Coventor, Inc. took an early interest in the modeling, but other pressures led to a termination of the expectations. On these points, a research project can clearly be more manageable if everything is 'under one roof'. However, a major thrust of the project was to study material from various sources and to involve industrial collaborators.

- This effort was enhanced by support from other organizations. The National Science Foundation has supported the experimental work of the senior PI, Sharpe, for many years and sponsored research into test methods for MEMS materials from 1993 to 2002. The Alexander von Humboldt foundation partially supported the 18-month postdoctoral fellowship of Dr. Joerg Bagdahn. The Korean Science Foundation partially supported the yearlong visit of Professor Oh. The Universitie de Paris partially supported the visit of Professor Dirras for eight months.

- Other MEMS materials could have been tested if specimens were available. But, these tensile specimens are relatively large and therefore expensive for a lab or foundry to produce. MEMS is a new technology, and the emphasis is naturally on new devices and applications. That will change as the field becomes more sophisticated and competitive and designers need to push the limits of material behavior.

- Correlating the microstructure with the material properties requires two things – test methods capable of determining differences and controlled variation of the processing. The first requirement is now met, but arranging with others to vary processes is perhaps asking too much. Much of process development is trial and error to achieve a particular goal, say low residual stress or smooth edges, and once a recipe is found, one is reluctant

to change it. For these reasons, the study of the property/microstructure relationship is not as complete as was hoped.

1.0 – Introduction

The broad objective of this project was to measure the mechanical properties of materials used in microelectromechanical systems (MEMS) and to relate their microstructure to the macroscopic behavior. This project built upon the experience of three Johns Hopkins University researchers in this area involving leading material manufacturers as well as experts in MEMS modelling at Microcosm, Inc. (now known as Coventor, Inc.). The initial plan was to receive material and specimens from MCNC (name changed to Cronos and then JDS Uniphase during length of project), Standard Microsystems Corporation, Pennsylvania State University, the Army Research Laboratory, Sandia National Laboratory, Case Western University, the Naval Surface Warfare Center, and MIT. As the project progressed the involvement of the various organizations listed above fluctuated for a variety of reasons requiring adjustments to the project as the various efforts tasks were pursued. Nevertheless, the researchers worked to measure the stress-strain curves of the most important MEMS materials over a range of temperatures, to develop techniques and procedures for measuring their fatigue and creep behavior, and to relate those properties to the underlying microstructure. This report provides an overview of what was accomplished during this effort and is organized according to the project tasks under which the research was performed. The MEMS community as a whole will now have better materials information to assist in the integration of the technology into new systems.

2.0 - Polysilicon stress-strain at temperature and CTE.

The original objective of this task was to tensile test polysilicon thin films produced at MCNC and Standard Microsystems Corporation at temperatures ranging from –40 to 600 ^{o}C. The CTE values and stress-strain curves were to be extracted from these experiments.

It is not surprising that most of the effort was devoted to polysilicon; it is still the most widely used MEMS material. The basic tensile test techniques and procedures had been developed prior to the start of the project, but it is useful to revisit the kind of results achieved. Figure 2.1 is a stress versus biaxial strain curve for a polysilicon specimen 3.5 µm thick, 600 µm wide, and 4 mm long. Although it is a ‘large’ specimen, it is manufactured at Cronos in the same process line as is used for MEMS. Note how linear the material is until sudden brittle fracture. Strain is measured in two directions by laser interferometry from gold markers on the gage section, and this has enabled the first measurements of Poisson’s ratio ever made on polysilicon.

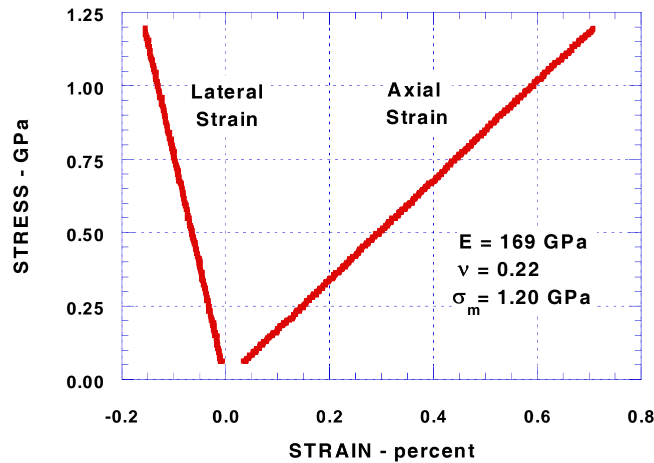

Figure 2.1 - Stress versus biaxial strain for polysilicon.

This capability permits one to compare various materials, and those results are shown in Figure 2.2. Polysilicon tensile specimens from three sources were tested for Young's modulus and fracture strength. These were narrow tensile specimens 50 µm wide and 0.5 to 2 mm long in contrast to the wider ones for Figure 2.1. Cronos and Sandia supplied specimens from their typical production runs. Standard MEMS Inc. (SMI) supplied material from two processes. It is interesting, and disconcerting, to note that Cronos had changed parent companies and SMI had decreased in activity in the three short years.

One would expect that the Young's modulus of a structural material would not vary with the manufacturing process, but that the strength would. All steels have essentially the same modulus, but widely varying strengths depending on alloying and heat treatment. That expectation is met in Figure 2.2 [1,2]. The modulus values are similar, but the fracture strengths vary by a factor of two. The strength difference is believed to result from different roughness of the specimen sidewalls.

Another point should be made relative to Figure 2.2. Note that many data points were taken for each material, in contrast to the few that are obtained for common structural materials. This is necessary to give statistical credence to the values because of the variations in the material itself and the uncertainties in the measurements.

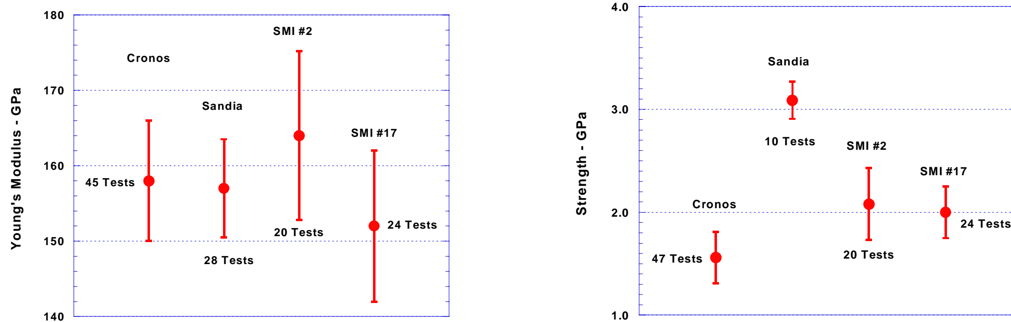

Figure 2.2 – Young's modulus and fracture strength for four materials [1,2].

David LaVan, then at Sandia-Albuquerque, arranged a limited 'round robin' of test methods for polysilicon [3]. The narrow specimens were 2.5 μm thick of various lengths and were all produced at the same time. They were tested at Hopkins, in Japan by Tsuchiya, and at Sandia; other initial participants were unable to complete the tests. The recorded strengths are shown in Figure 2.3.

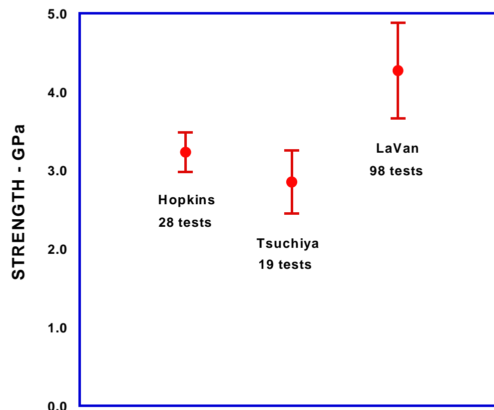

Figure 2.3 – Comparison of strengths of Sandia polysilicon measured in three laboratories [3].

The Hopkins and Tsuchiya results are close to each other, considering the scatter as indicated by the standard deviation markings. LaVan's results are quite a bit higher. He used a nanoindenter with a side-loading transducer to record the breaking force of specimens with a ring on their grip end. The probe was inserted into the ring and the specimen pulled to failure. It is now believed that friction between the probe tip and the substrate may have contributed to the high values. Nevertheless, it is reassuring to note that similar results are obtained from laboratories in different countries.

In addition to these important results at room temperature, this task considered the effect of temperature on the mechanical behavior of polysilicon. Tensile testing at high temperature

introduces complications, and two approaches were taken. First, specimens were heated in a small resistively heated furnace with a quartz window to permit optical access for strain measurement. The second approach heated wide specimens by passing current through them [4,5].

Figure 2.4 shows the decrease in Young's modulus with increasing temperature for the two approaches. The upper limit is 250°C because the gold markers began to deteriorate at that temperature.

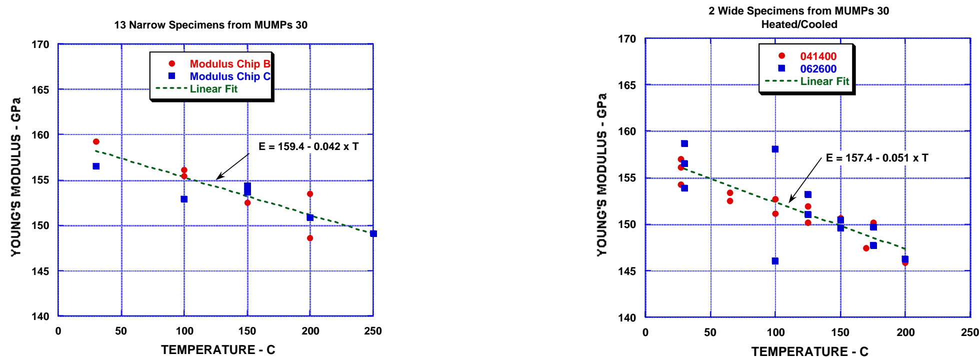

Figure 2.4 – Variation in Young's modulus with temperature for polysilicon [5].

The variation is essentially the same for both kinds of specimens and does agree in general with limited earlier research by others. This may seem like an insignificant effect, but a small change in modulus can generate large stresses in restrained components. The fracture strengths of these specimens showed no significant change with temperature.

Whereas these results are useful for microdevices operating in this temperature range, e.g. automotive components, a more interesting response occurs at the higher temperatures experienced by thermal actuators. They glow red, and testing at such high temperatures is a considerable challenge, especially the strain measurement. The wide specimens can be heated resistively to red-hot, and temperature can be measured with an optical pyrometer. If the gold reflective markers are replaced by platinum ones, then strain can be measured directly on the specimen by the laser interferometry method. Platinum lines were deposited on the specimens by the Northrup Grumman Advanced Technology Laboratory in Baltimore with the cooperation of Dr. Carl Freidhoff, a fellow DARPA contractor. Figure 2.5 is a photograph of a heated polysilicon specimen; the temperature distribution in the center section was modeled by Microcosm, Inc under the thin film modelling task. The platinum lines are visible in the center and are seen to be a bit offset due to an error in processing.

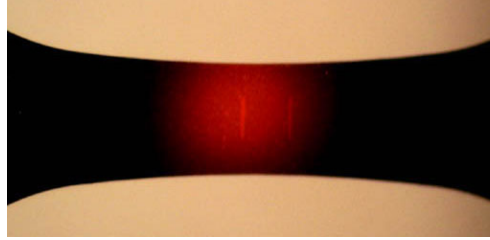

Figure 2.5 – A 600 µm wide polysilicon specimen at 600°C.

Figure 2.6 shows two aspects of high-temperature stress-strain behavior. The plot on the left compares the mechanical response at 670°C to that at room temperature. Polysilicon becomes inelastic and its strength is greatly reduced. The plot on the right shows the stress-strain curve at 700°C. The polysilicon is deforming very easily at that high temperature; note the immediate relaxation and creep when the loading is stopped.

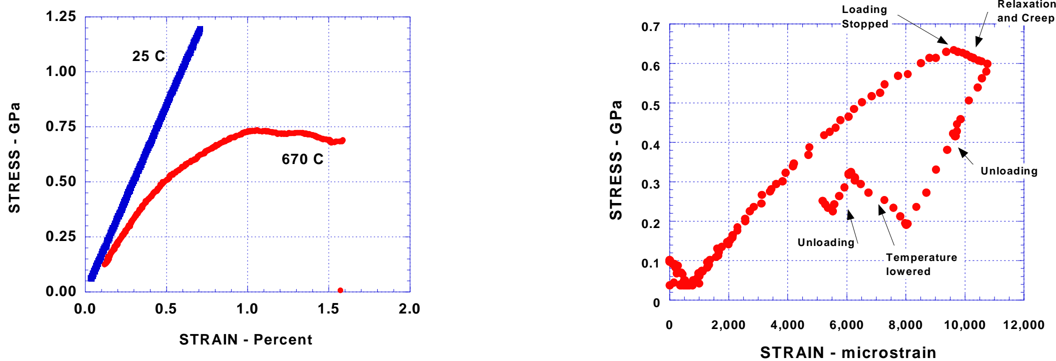

Figure 2.6 – Polysilicon at 25°C and 670°C (left) and 700°C (right).

Perfection of these test methods occurred in the last third of the project. Application of the platinum lines by Northrup Grumman was done gratis, but subject to their other priorities and hence often delayed. The major outcome of this part of the research is establishment of the test methods and setting the temperature ranges of interest for future studies.

The thermal coefficient of expansion of polysilicon is an important physical property, and it assumed in virtually all applications to be the same as single crystal silicon. That is reasonable given the cubic structure of silicon, and the value of 2.9×10^{-6}/°C is often used. One would expect a similar value for polycrystalline silicon, but measurements show a higher value on the order of 4×10^{-6}/°C. This has been troubling, but several different approaches have been taken with essentially the same results. Figure 2.7 shows the measured thermal strain versus temperature and compares it with handbook values for silicon.

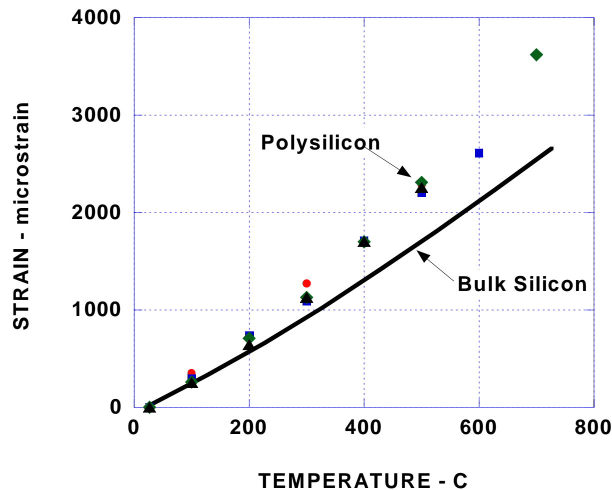

Figure 2.7 – Measured thermal strain for polysilicon (data points) compared with bulk silicon (Thermophysical Properties of Matter, Volume 13, Y. S. Touloukian, Editor, IFI Plenum Press, page 154, 1977).

The measured strains are higher and exhibit the same upward curvature as the single crystal material. Other researchers have reported higher values, but no definitive results exist. These are believed to be accurate, but it is still troubling that no microstructural explanation is available. Researchers at Case Western Reserve University have stated that this polysilicon from Cronos has oxide in the grain boundaries, but have provided no concrete details. That could be an explanation for the higher expansion.

An important addition to the research program was suggested and then carried out by Dr. Bagdahn. Mechanical failures, whether they are from fatigue or overloading, invariably initiate at stress concentrations. In fact, most of mechanical structural design centers around finding the ‘hot spots’ in a component where the stresses are highest and then adjusting the loading, geometry, or material to meet a failure criterion. The same approach must be taken for MEMS, but it is more complicated when the material is brittle. The local stresses can be calculated from a finite element analysis and for ductile materials must simply be smaller than the yield strength of the material by a suitable factor of safety. Not so for brittle materials; as the volume or surface area gets smaller, the strength actually increases because of the decreased probability of a fatal flaw [6].

Dr. Bagdahn designed specimens as shown in Figure 2.8 [7,8]. The straight specimen is regarded as the ‘baseline’ one, and the other two have readily determined stress concentrations. These were made at JDS Uniphase (formerly Cronos) and were 3.5 μm thick and either 20 or 50 μm wide. They were loaded in tension and only the fracture strength was measured. The radiuses of the hole and the notches are 2.5 μm, which is close to the minimum feature radius of most MEMS processes.

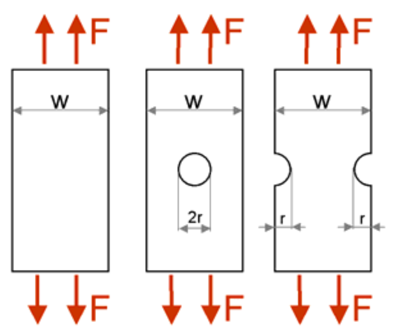

Figure 2.8 – Schematic of the notched specimens.

A new description, Weibull statistics, is needed to accurately handle this different phenomenon. Dr. Osama Jadaan of the University of Wisconsin – Platteville and NASA Glenn Research Center collaborated on the analysis. NASA has an intense interest in brittle ceramics for engine materials and has assembled considerable expertise. Details are given in a recently accepted JMEMS paper, but the concept is to take the results from the straight specimens and, in conjunction with a finite element analysis that incorporates Weibull statistics, predict the failure of a notched component. A result is shown in Figure 2.9 where the predicted solid line shows a slightly higher (and conservative) probability of failure than actually occurs [9].

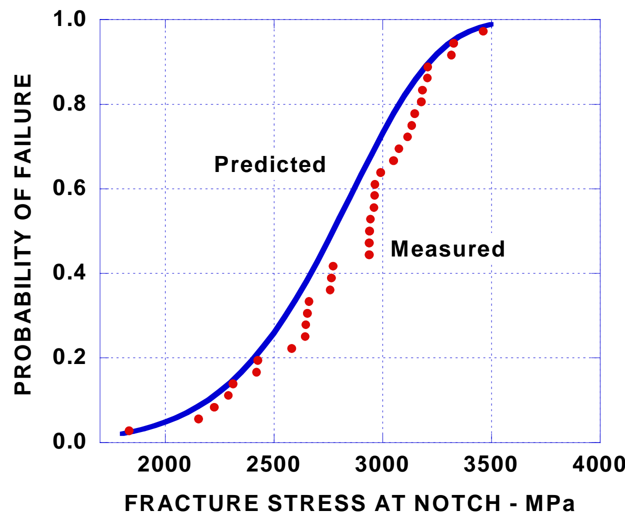

Figure 2.9 – Predicted versus measured fracture stresses for
a double-notched specimen 20 μm wide.

These results show that the approach works, but clearly extensive testing would be needed for a material and a manufacturing process.

3.0 – Case Western silicon carbide.

Microsample tensile specimens of silicon carbide (SiC) thin films from Professor Mehregany of Case Western Reserve University were prepared in a manner similar to the way that polysilicon microsamples were made. These specimens were used to obtain stress-strain curves and CTE values will be obtained at temperatures ranging from room temperature (RT) to 600 ^{o}C.

SiC is a promising MEMS material because of its expected strength at high temperatures and resistance to chemical attack. A thin-film version is undergoing continuing development at Case Western Reserve University (CWRU) by Professors Mehregany and Zorman. Their research was sponsored by the same DARPA program, and they collaborated on the mechanical property measurement by providing specimens. This activity was a major part (roughly one half) of the thesis research of now-Dr. Kamili Jackson.

This brand of silicon carbide is produced by vapor deposition in much the same manner as polysilicon. It took considerable effort on the part of CWRU to finalize a process that produced clean specimens with low residual stresses. Depositing the reflective markers for strain measurement was also an issue, and the final version uses platinum lines because that material was available. Etching the window into the back of the silicon die and mounting the specimen followed the same procedures as for polysilicon, and a specimen ready for testing is shown in Figure 3.1 [10].

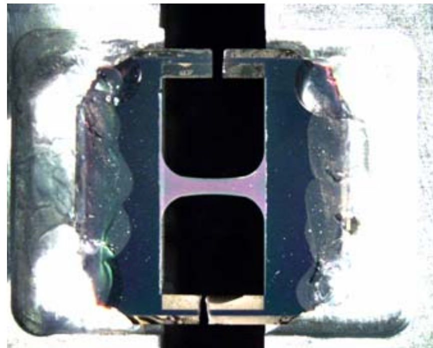

Figure 3.1 – A silicon carbide specimen from CWRU; it is 0.5 μm thick.

The stress-strain curve in Figure 3.2 is uniaxial only. Lines were deposited for lateral strain measurement, but a slight bowing of the specimens after release rendered them unusable. The curve is not as smooth and straight as for polysilicon, which shows the difficulty in preparing this material for test.

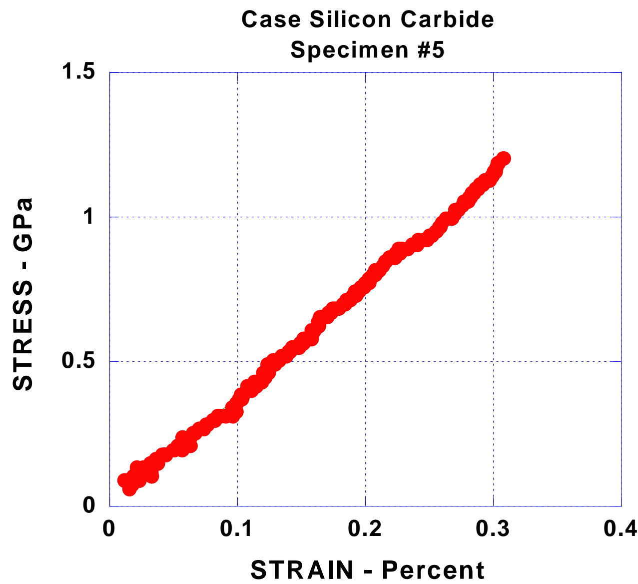

Figure 3.2 – Stress-strain curve for CWRU silicon carbide.

Batches from two different runs of CWRU silicon carbide were received, and the cumulative results are presented in Table 3.1 [11].

Table 3.1 – Properties of CWRU silicon carbide.

	Number of tests	Young's modulus GPa	Number of tests	Fracture strength GPa
Batch one	14	410 ± 45	35	1.10 ± 0.48
Batch two	8	435 ± 41	25	1.65 ± 0.39

The global average for the modulus is 428 ± 42 GPa, which is within the range obtained for bulk material. The large scatter in the strength values and the variation between the two processes is alarming. Silicon carbide is a brittle material, and the smoothness of the surfaces is important. Processing of microdevices may be different from processing of specimens, but clearly the uncertainty in the strength is a major concern.

4.0 – Other thin-film materials.

Originally the task covered in this section of the report was supposed to examine lead-zirconium-titanate (PZT) specimens. At the time of the proposal, the Army Research Laboratory (ARL) was trying to manufacture wide tensile specimens of PZT by the thin-film sol-gel deposition process. Residual stresses are generated and even though the 0.5 μm thick PZT was sandwiched between 0.1 μm thick layers of platinum/titanium, the specimens still fractured during the release process. The processing facilities at ARL were in a state of flux at the time because of a move from Fort Monmouth, NJ to Adelphi, MD. The effort for this particular task was refocused since the DARPA project had attracted an interest in other materials. The task was modified to examine tensile specimens of thin-film materials that were not part of the original proposal and were provided from other sources. Examples of such materials are: silicon-germanium from the Berkeley Sensor and Actuator Center, silicon nitride from both Northrup Grumman and Goddard Space Flight Center, and thicker polysilicon from Analog Devices. It is ironic that ARL has been able to produce much better specimens in the last few months of the project, but the interaction will now have to continue separate from this effort.

Silicon nitride

NASA Goddard uses silicon nitride as supporting structures in their bolometers; the temperature-sensing element is raised above the substrate for thermal isolation. They supplied 0.5 μm thick film on wafers, which were patterned into wide specimens at APL. A photo of one of the specimens is shown in Figure 4.1 where the deposited gold lines for strain measurement are clearly visible.

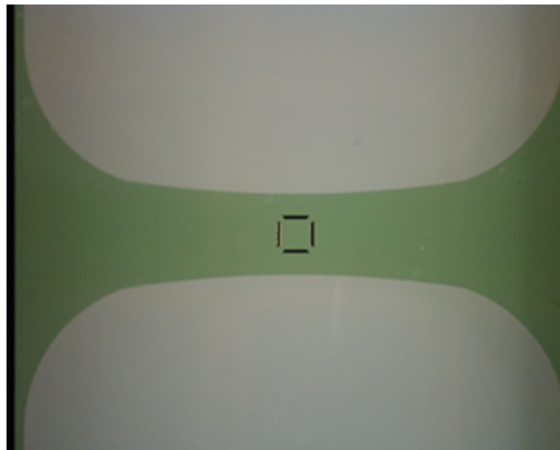

Figure 4.1 – A silicon nitride specimen. It is 0.5 μm thick and 600 μm wide.

Testing these is similar to the polysilicon material and is easy in spite of the reduced thickness. A typical stress-strain plot is in Figure 4.2. It is similar to Figure 2.1, but note that silicon nitride is stiffer and much stronger [12].

The cumulative results from a set of 13 tests yield the following properties of silicon nitride – Young's modulus = 255 ± 2.6 GPa, Poisson's ratio = 0.22 ± 0.02, fracture strength = 6.42 ± 1.11 GPa. The larger scatter in the strength values is probably due to sidewall variations.

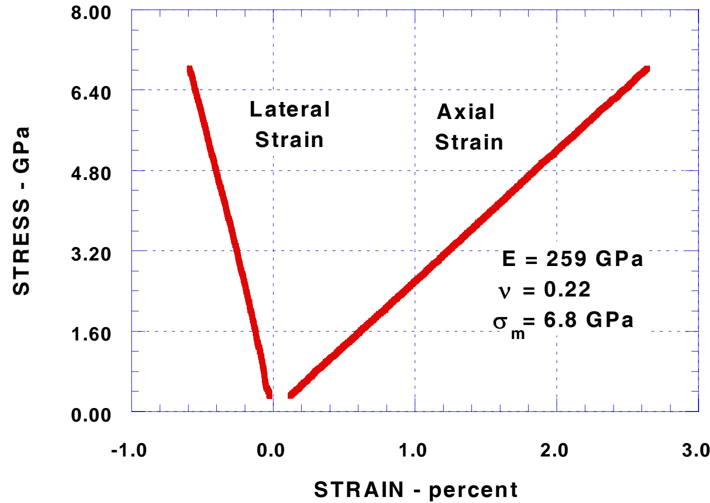

Figure 4.2 – Stress versus biaxial strain for silicon nitride.

Test method comparison

The semiannual DARPA meetings led to an important collaboration with Dr. Stuart Brown of Exponent, Inc., who was a participant in the same program. His interest was in on-chip test methods, and he uses a one mm square membrane for a bulge test. The obvious step was to compare mechanical properties obtained from tensile tests to those from bulge tests. Silicon nitride was the material chosen, and tensile and bulge specimens were fabricated – all on the same wafer – at APL [13,14]. A photograph of the two kinds of specimens is in Figure 4.3

Table 4.1 presents the compared results. The modulus agreement is exceptional, but note that the tests were conducted independently at two facilities. Tensile tests have the advantage of providing values of Poisson's ratio and strength; whereas, bulge tests can measure the residual stress in the film.

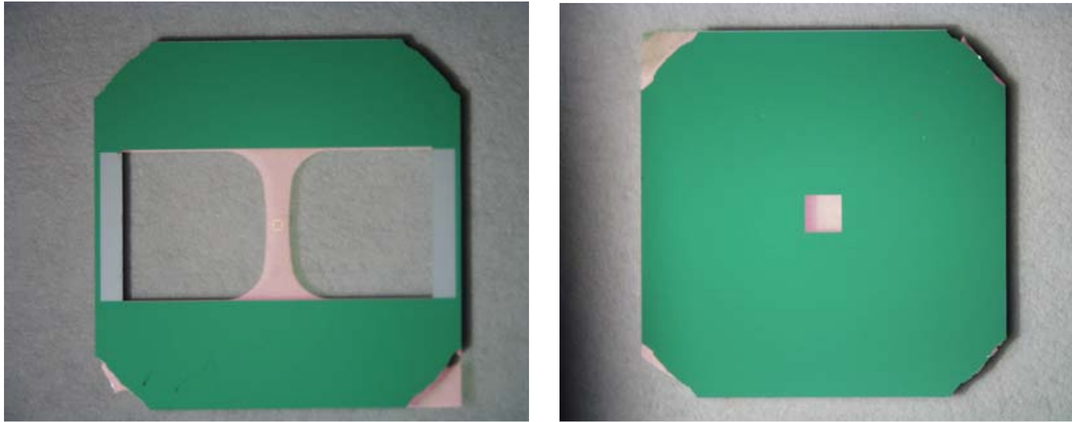

Figure 4.3 – A tensile and a bulge test specimen of silicon nitride.
The die is one cm square in each case.

Table 4.1 – Results from comparison tests.

	No. of tests	Modulus GPa	Poisson's ratio	Strength GPa	Residual stress - GPa
Hopkins	7	257 ± 5	0.22 ± 0.03	5.83 ± 0.25	NA
Exponent	3	258 ± 1	NA	NA	114 - 130

This exercise illustrates another aspect of the value of this work. If tensile tests are regarded as the standard test method, they can be used to validate a different test method, which has the advantages of permitting on-chip testing.

Silicon Germanium

Silicon germanium is a promising MEMS material because the processing temperatures are lower. The Berkeley Sensor and Actuator Center is developing this material and has supplied specimens. A single tensile specimen on a die is pictured in Figure 4.4.

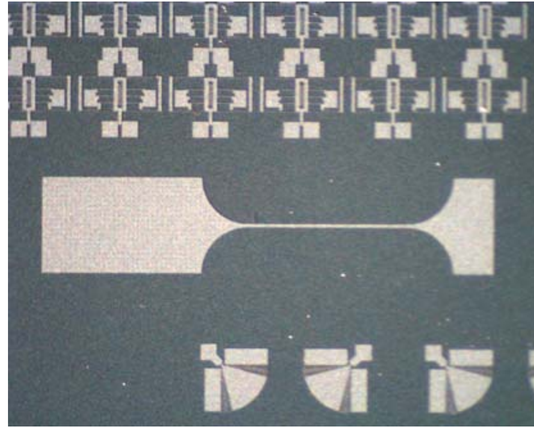

Figure 4.4 – A silicon germanium specimen on a die with other microdevices.

This photograph demonstrates one of the issues in soliciting test specimens from laboratories. The tensile specimen is much larger than the resonator specimens at the top or bottom. Those can be used to determine elastic properties in an indirect manner, but cannot provide strength values. The relatively large size of the tensile specimen makes it quite expensive, which explains the difficulties in obtaining specimens in spite of the best intentions of the providers.

Residual stresses in the initial version of this material were large, and when the grip end at the left in Figure 4.4 was released, the specimen curled. That was no particular problem; the grip end was pushed back down with a micromanipulator and a fiber glued to it. A result is shown in Figure 4.5.

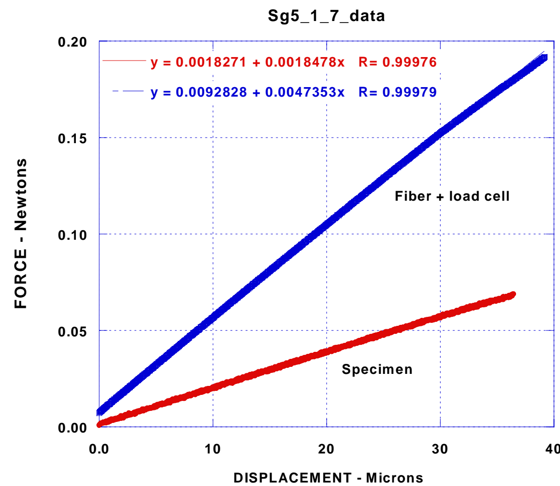

Figure 4.5 – Force versus displacement for a silicon germanium specimen.

The displacement in the lower curve labeled ‘Specimen’ is the sum of the elongation of the specimen plus the grips and the displacement of the load cell. The upper curve was obtained after the specimen had broken and its grip end glued back to the substrate. In theory, one should be able to subtract one from the other and determine the modulus of the specimen material. That is not very accurate because of unknown deformation in the adhesive; this demonstrates the value of direct laser-based strain measurement.

The strength was measured for seven specimens with an average value of 1.07 GPa and a range of 0.78 to 1.32 GPa. No further tests were conducted.

CMOS material

The concept of fabricating mechanical components directly in CMOS layers is attractive because of the easy integration of the electronics with the mechanical components. This study was initiated by Dr. Bagdahn in collaboration with Professor Fedder of Carnegie Mellon – also as a result of the DARPA semiannual meetings. Figure 4.6 shows a die containing several types of tensile specimens.

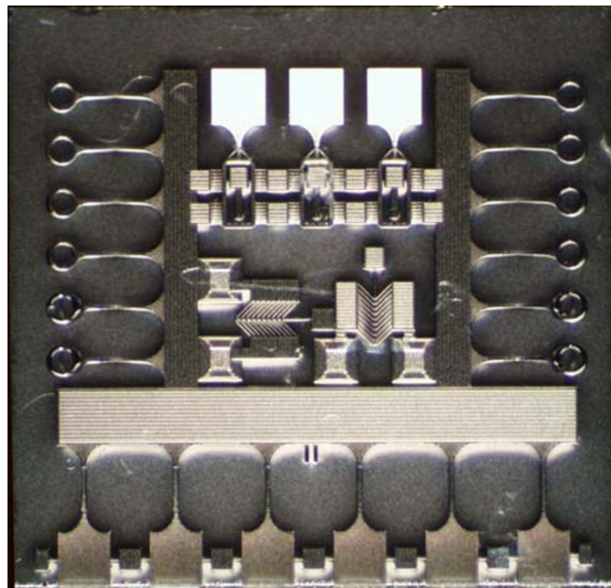

Figure 4.6 – CMOS tensile specimens and thermal actuators on a die from Carnegie Mellon.

The tensile specimens with the large solid grip ends are similar to other narrow ones, and a fiber would be glued to them. The ones on the sides have rings at the ends for easier gripping, and these turned out to work quite well, and results are shown in Figure 4.7 [15]. The middle structures are small thermal actuators to demonstrate a proof-of-concept.

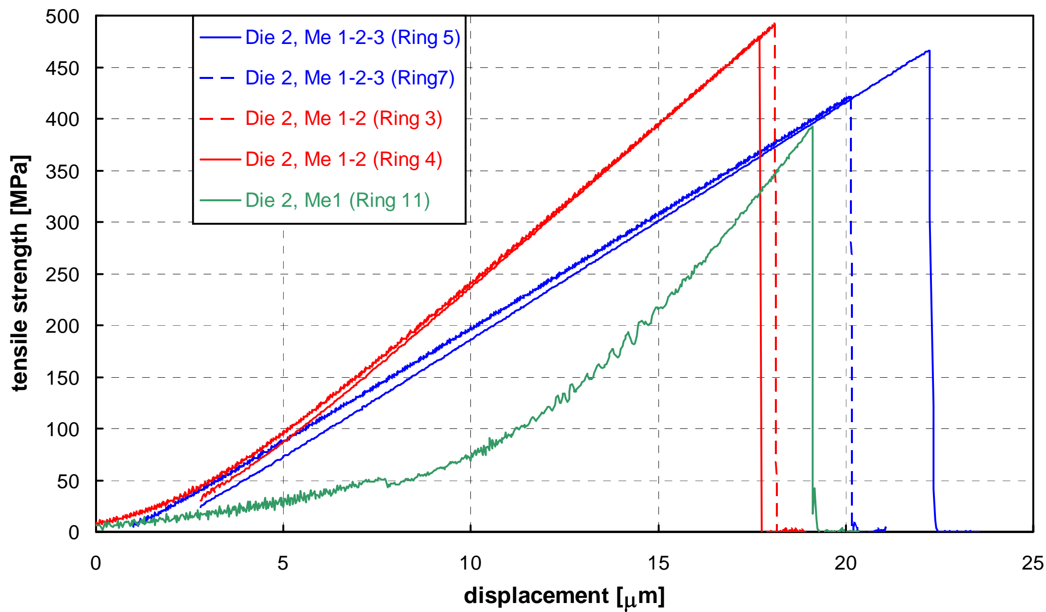

Figure 4.7 – Stress versus displacement for CMOS specimens with different layers.

The two plots labeled 'Me 1-2-3' are the full three layers of aluminum and three layers of glass. Those labeled 'Me 1-2'are two layers of each, and the 'Me 1' is one layer of each. The thicker specimens show linear behavior after an initial curvature, but the single-layer one takes a higher stress to straighten out. CMOS material has quite high residual stresses (all the specimens were curled up from the substrate after release), so the initial behavior is quite complicated. Note that the fracture strengths are lower than other materials at about 0.4 GPa, but this is still a respectable value. Failure was observed to initiate in the glass layer in all cases.

<u>Silicon carbide from NASA Glenn</u>

In the course of presentations of this research, Mr. Noel Nemeth of NASA Glenn became interested in testing materials under development there. They have been a leader in developing deposition processes for both single-crystal and polycrystalline silicon carbide and are exploring applications of it in engine components. They are supplying large microspecimens, and to be tested for strength only. This work is funded separately at a modest amount and will continue into 2003 to take advantage of the expertise in testing at high temperatures.

5.0 – Diamond stress-strain curves.

At the time the proposal was written, Drs. Sullivan and Friedman of Sandia-Albuquerque were producing amorphous diamond films with low residual stresses and agreed to supply

amorphous diamond films for microsample testing. Stress-strain curves of this material were obtained at RT.

Diamond (really amorphous carbon) MEMS are attractive because of the expected high modulus and low coefficient of friction. Sandia-Albuquerque is a leader in developing these materials and provided specimens. Figure 5.1 is a photograph of a die containing various shapes of tensile specimens; the narrow ones with large paddle grips were the ones of interest.

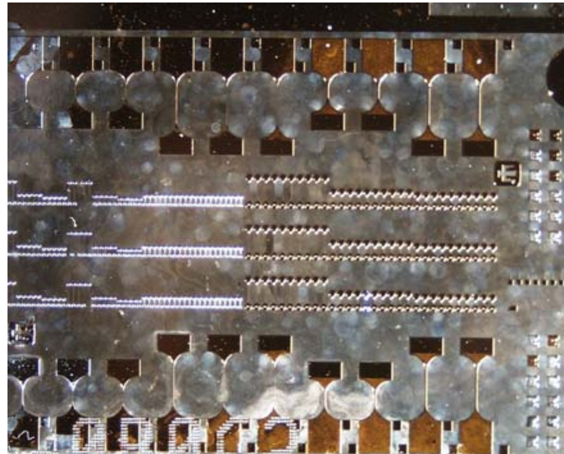

Figure 5.1 – Diamond specimens from Sandia.

It is not obvious from the picture, but some of the specimens are not fully released. However, fibers could be glued to the paddle as shown in Figure 5.2.

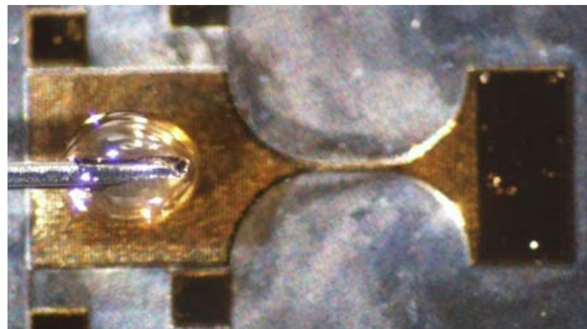

Figure 5.2 – A diamond tensile specimen with fiber attached. The test section is 1.5 μm thick, 20 μm wide, and 250 μm long.

A stress versus displacement plot is presented in Figure 5.3. The displacement is that of the entire system including the adhesive, the fiber, and the load cell. A record of force versus

displacement after the specimen failed was also taken to attempt a calculation of the modulus – same as in Figure 4.5.

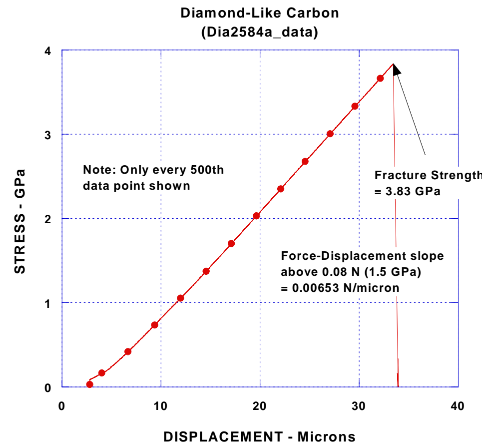

Figure 5.3 – Stress versus displacement for diamond.

Twelve tests were conducted and yielded a fracture strength of 3.7 ± 1.4 GPa and a Young's modulus of 606 ± 147 GPa. The large scatter in the modulus renders them suspect, since the contribution from the adhesive is unknown. The even larger scatter in the strengths may be due to either the material or the test method. This is as far as could be gone with the specimens available. However, it does show that tensile tests can be conducted. A concentrated effort that included direct strain measurement on larger specimens would have a high probability of success.

6.0 – Polysilicon fatigue

The fatigue test effort was an outstanding success, thanks to Dr. Bagdahn [16,17] who developed a new test method for tensile fatigue and tested many polysilicon specimens.

Specimens were tested in a unique facility using, in the final version, a small loudspeaker to drive the specimen at 6000 Hz. A photograph is shown in Figure 6.1. The specimen is the narrow type, and a fiber is glued to the grip end. The other end of the fiber is connected to the center of the loudspeaker (piezoelectric actuators were used at lower frequencies as the system was developed). The die containing the specimen is glued to a small block attached to a piezoelectric actuator capable of measuring force at 6 kHz.

The results are presented in Figure 6.2. The increase in fatigue life as the applied stress is reduced is typical of metals, but not brittle ceramics. This overall behavior has been observed by others using resonant specimens with more complicated stress fields. The microstructural mechanisms to explain this are still missing, but it appears that the oxide on the surface thickens with cyclic loading and then cracks.

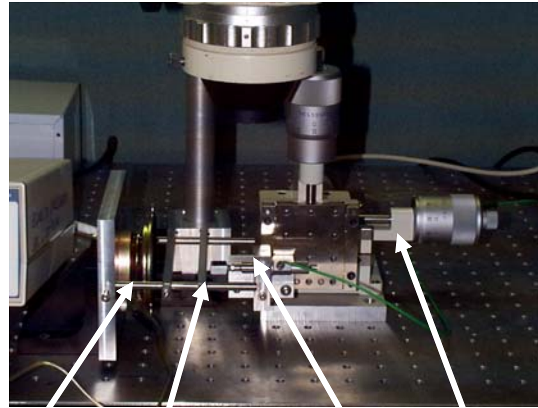

Loudspeaker   Specimen on die   Load cell   Three axis stage

Figure 6.1 – Photograph of the fatigue test setup.

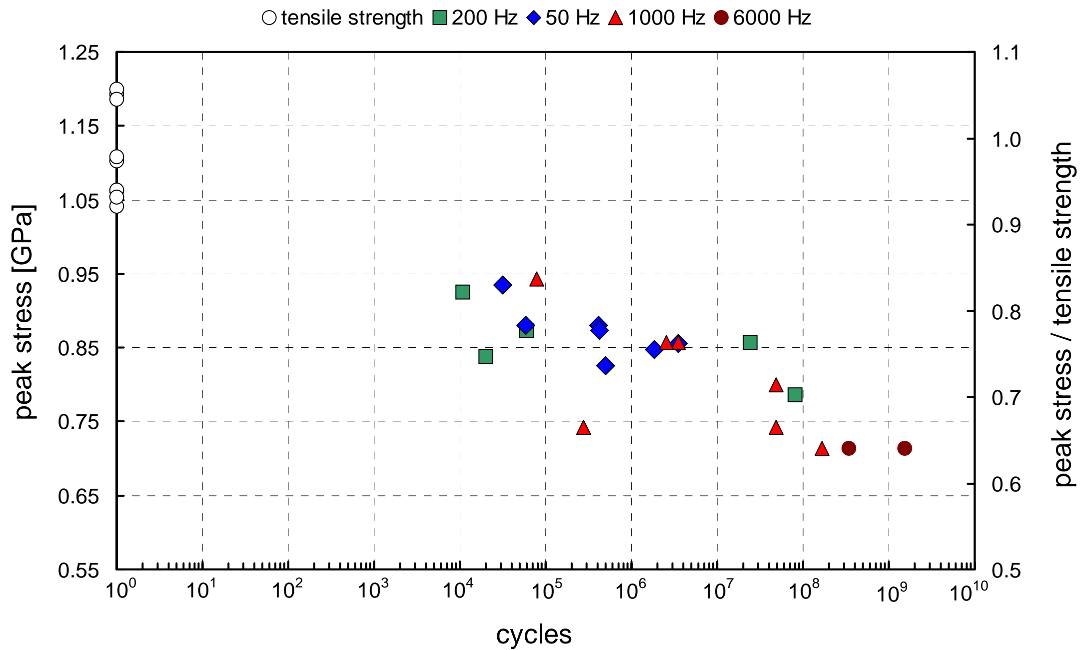

Figure 6.2 – Stress versus number of cycles to failure for polysilicon.

One should note that the data points in Figure 6.2 were obtained at different test frequencies – increasing as the test method improved. The fact that the results are independent of test frequency implies that stress corrosion is not a factor in the fatigue of polysilicon.

However, specimens were tested in ‘static fatigue’, i.e. a constant force is applied and the time to failure is measured. This required a special setup in which the force was maintained through a feedback loop incorporating a piezoelectric actuator and a load cell. Figure 6.3 shows those results, which contradict the lack of stress corrosion effect. The specimens with lower applied stresses lasted longer and those in a water environment clearly failed earlier than the ones in laboratory air.

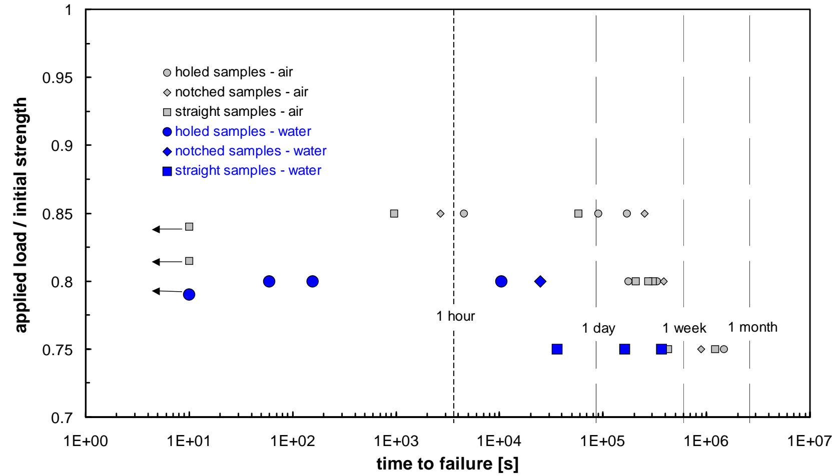

Figure 6.3 – Static fatigue results for polysilicon in air and water.

Obviously more research is needed on this topic, but this work sets the stage both in terms of test method and results.

7.0 – Polysilicon creep

The objective of this task was to develop experimental methods for conducting high temperature constant load creep tests and measure the creep response of polysilicon films. Tests would then be conducted at a variety of stresses and temperatures and the results from these tests used to characterize the creep behavior of this material in terms of thermally activated deformation processes.

Wide polysilicon specimens can be heated resistively as shown under Task 1, and they can then be subjected to creep loading. This turns out to be not so difficult, but specimen preparation, which involves depositing platinum lines with a Focused Ion Beam machine, is time-consuming and expensive. Figure 7.1 shows the creep behavior under four conditions; they serve to bracket the temperature and stress range for future testing. It is clear that polycrystalline silicon behaves much like a ductile metal in this regime.

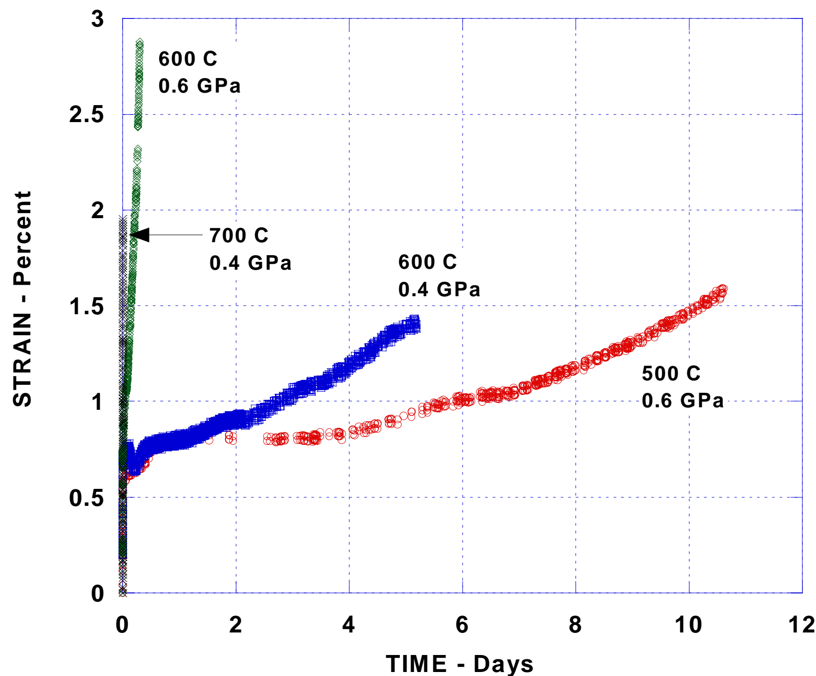

Figure 7.1 – Creep behavior of polysilicon at different temperatures and loads.

Professor C-S Oh was visiting from Korea and has designed a new test method for creep. The specimen is of the narrow type, and a picture is shown in Figure 7.2. The rectangles at the ends of the gage section are for vernier measurements, but they have proved ineffective. The adhesive bond looks easy, but was very difficult to achieve. It is hard to find an adhesive that will withstand 800°C and yet be viscous enough to not penetrate the etch holes in the grip.

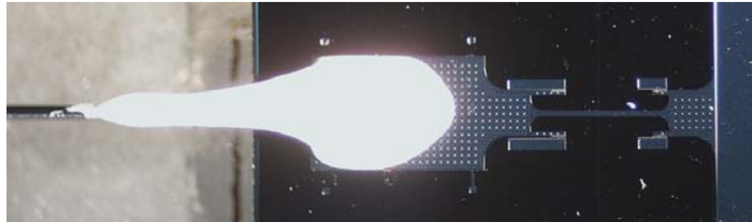

Figure 7.2 – Photograph of a narrow creep specimen with a fiber glued to the grip end.

The advantage of the narrow specimens is that they are cheaper initially in that one gets more per die. The entire operation from gluing the grips to placing the assembly in a vertical furnace is very delicate. Strain can be measured directly from platinum lines on the gage section, and Figure 7.3 shows that the results from this test method agree well with those from a wider specimen.

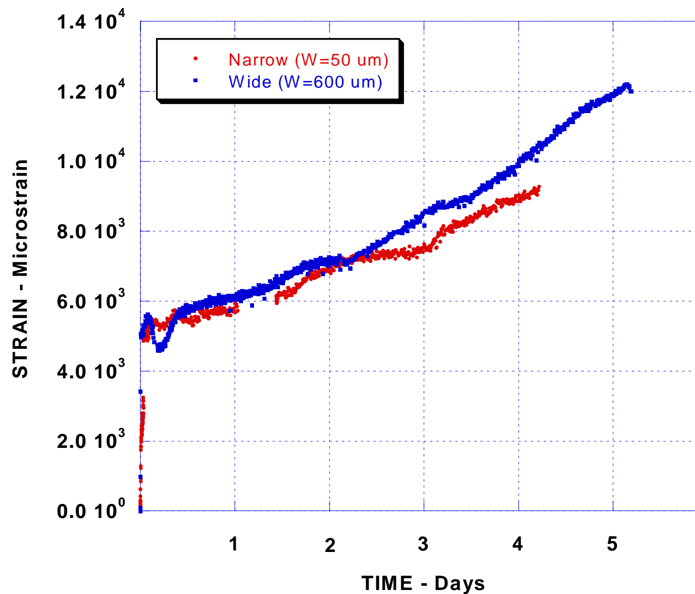

Figure 7.3 – Creep results for a wide and a narrow specimen at 600°C and 0.4 GPa.

This research continued on after the agreement ended since Professor Oh was scheduled to be at JHU until February, 2003, and some more fully prepared specimens had been received.

8.0 – Thin film microstructural studies.

Microstructural studies were initiated immediately and continued throughout the project. Thin-film MEMS materials are often deposited under conditions that are far from equilibrium and microstructural observations are needed to correlate the measured mechanical properties with the as-deposited microstructures. The usefulness of optical metallography will be limited by the fine structure associated with the thin film materials, but Scanning Electron Microscopy (SEM) and Transmission Electron Microscopy (TEM) observations and x-ray analysis will be used to identify grain size, grain distributions, and texture, as well as, active deformation and fracture processes.

The microstructural studies of thin film materials were focused on polysilicon and SiC. As described in Section 2.0, polysilicon specimens made by three different vendors (Cronos, Standard MEMS, and Sandia) have been found to have significant differences in tensile (fracture) strength. Considerable effort was spent searching for a microstructural explanation for this difference in strength. The main findings of this study are outlined below, but the conclusion was that there is no clear microstructural or chemical difference in the three different versions of polysilicon. However, low magnification TEM observations of the edges of polysilicon films specimens manufactured by Cronos, Standard MEMS, and Sandia suggest that the Sandia specimens have significantly lower surface roughness. This observation would explain the results that the tensile strength of Sandia polysilicon is significantly greater than that for the Cronos or Standard MEMS samples. Attempts to quantify this observation have been hindered by the fact that a sufficient quantity of the Sandia specimens was not available.

The observations of polysilicon tensile specimens can be summarized as follows [18]. The microstructures of polysilicon thin films supplied by Cronos and Standard MEMS *Inc*. (SMI) have been analyzed. The microstructural investigation included: (i) conventional TEM, (ii) texture determination by x-ray diffraction and/or electron back scattering diffraction pattern (EBSP), (iii) SEM and Atomic Force Microscopy (AFM), and (iv) chemical analysis by use of the Auger Electron Spectroscopy (AES). The results are briefly summarized below.

(i) Conventional TEM characterization

Conventional TEM cross sectional investigations allowed us to qualify the grain morphology and the grain size in both materials. The Cronos samples exhibited fully columnar grains –along with a few small equiaxed grains– with boundaries perpendicular to the film surface although some deviations from this orientation were seen. Stacking fault (SF) like twins were also observed within the grains. Small equiaxed grains and very few columnar grains characterized the as-deposited SMI thin films. Smaller-sized nuclei were seen localized in the vicinity of the boundary between two layers or at the bottom of the sample where the grain growth starts. Cronos and SMI samples showed quasi-similar grain size, ranging from 0.2 to 0.35 μm (not taking in account the nuclei located at the boundary layer, which are nanometer sized). This is in contrast to Sandia thin films, which have been reported to have a slightly larger grain

size of approximately 0.5 μm (D. LaVan of Sandia Labs). This difference in grain size is not, however, enough to account for the difference in properties.

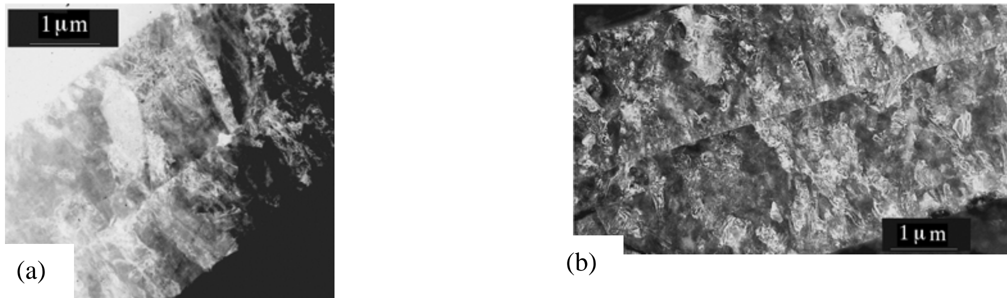

Figure 8.1 - TEM micrographs of (a): Cronos (MUMPS 25) and (b): SMI Polysilicon Thin Films

(ii) Texture analysis

Texture studies have been conducted on Cronos samples and compared with the data for Sandia thin film reported by D. LaVan. Both EBSP and X-ray diffraction were used to characterize the Cronos films. However, the first technique was limited by the small grain size. The results from the X-ray diffraction show that the columnar grain structure has a {110} texture as can be seen in the figure below. This is in contrast with the quasi-random texture reported in Sandia samples (D. LaVan of Sandia Labs).

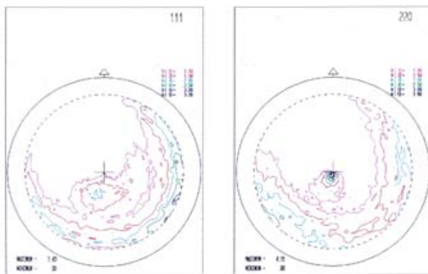

Figure 8.2 - {111} and {110} contours level of the x-rayed Cronos sample showing that {110} planes are parallel to the film surface.

(iii) Roughness Characterization of Cronos and SMI thin Films

SEM and TEM studies were conducted to investigate both the rupture surfaces and the microstructure of as-fabricated and tested polysilicon MEMS materials. The SEM micrograph in Figure 8.3 shows an abrupt-like failure. A closer observation indicates the presence of multiple flaws along the lateral surfaces of the sample. It is possible that the failure has been initiated from one of these flaws at the side surface of the sample. In a parallel study, atomic force microscopy (AFM) was used to study the surface roughness of both the top and side surfaces.

Measurements on the side surface proved to be elusive as it proved to be impossible to place the tip of the AFM on the ~3 micron thick film without breaking it. Observations of the top and bottom surfaces indicated that they are very smooth, as can be seen in Figure 8.4. The measured standard deviations of the top and bottom surfaces were on the order of 20 nm for the Cronos samples and 10 nm for SMI.

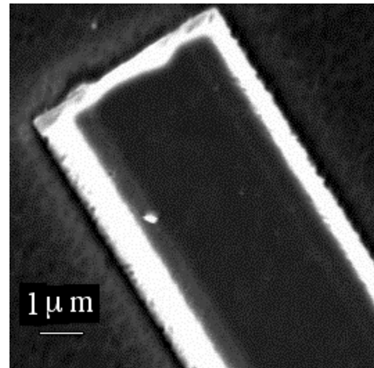

Figure 8.3 - SEM micrograph of the fracture surface of a polysilicon

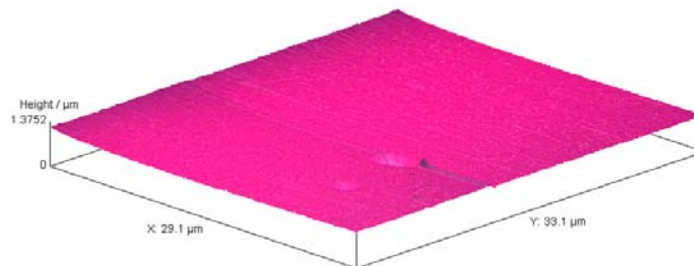

Figure 8.4 - AFM profile of the top surface of a polysilicon sample. Note that the visible discontinuity is an etch hole; the overall surface of the sample was found to be extremely smooth.

(iv) Chemical analysis

The chemical analysis of the samples was initiated using the AES. In this technique, an incident beam irradiates the sample and core electrons are ejected with a characteristic kinetic energy. Moreover the sputtering capability associated with AES permits to access to the depth profile of the elements of interest. Only preliminary studies were conducted, but no discernable difference was noted between the different specimens.

The microstructural observations of silicon carbide were made to compliment the studies reported in Section 3.0. Plan and cross-sectional view TEM observations showed a microstructure dominated by a very high density of twins. The grain boundaries were often difficult to distinguish from the twin boundaries when looking at the cross section, but the diameter of the columnar grains was determined to be between 0.15 and 0.2 5μm, see below.

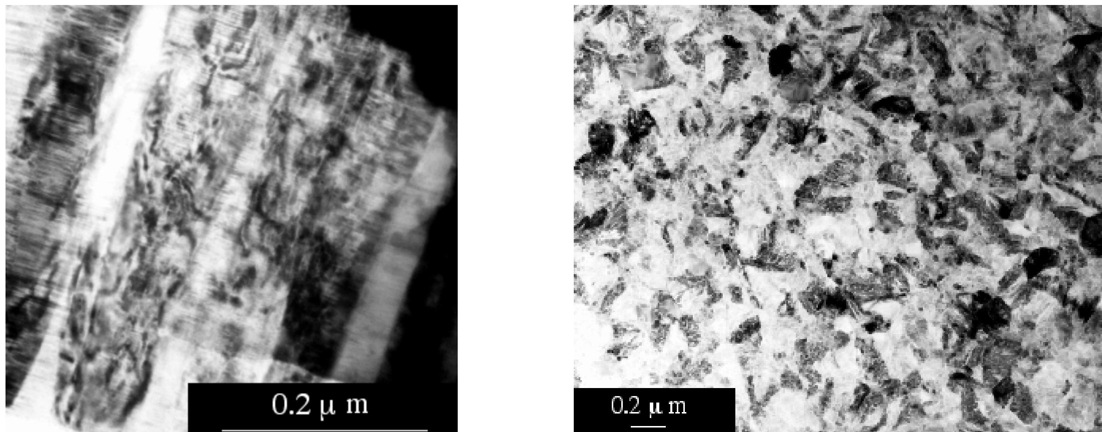

Figure 8.5 - TEM cross-sectional (left) and top view of the as-received SiC thin film.

The X-ray diffraction experiment revealed a cubic crystal structure, which was confirmed by TEM diffraction analysis, and a strong <111> fiber texture perpendicular to the film surface, as is shown in the pole figures below.

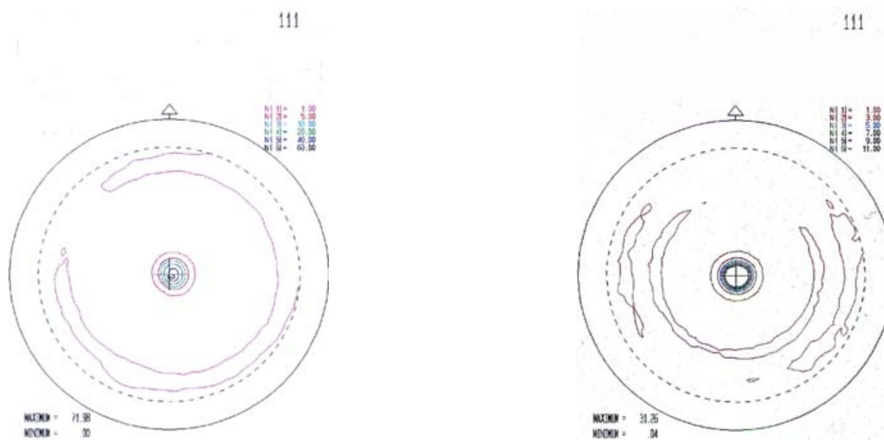

Figure 8.6 - Texture Evolution of SiC Thin film. 1: as received; 2: heat-treated @ 200°C-2h, showing the scattering of the <111> fiber.

9.0 – Modeling of thin films.

The original plan was for Drs. Bart and DaSilva of Microcosm to use their in-house MEMCAD tools to perform analysis and simulation of the thin-film materials tested in this study. Much of the modeling by Microcosm was planned to occur early on as the specimen design was refined. The remaining modeling effort would be distributed throughout the length of the project because analysis of test results would also use the models.

Microcosm, Inc. (now Coventor, Inc.) collaborated during the first year on modeling the temperature distribution in the resistively heated wide specimens and on the stress distribution in the Sandia polysilicon specimens. The latter effort was prompted by some peculiar failures in the grip ends, which turned out to be limited to that particular design and was not pursued further. The temperature distribution is important so that the uniformity of the temperature field in the central gage section can be assessed. Their model is compared in Figure 9.1 with temperatures measured with an optical pyrometer scan along the length of the specimen.

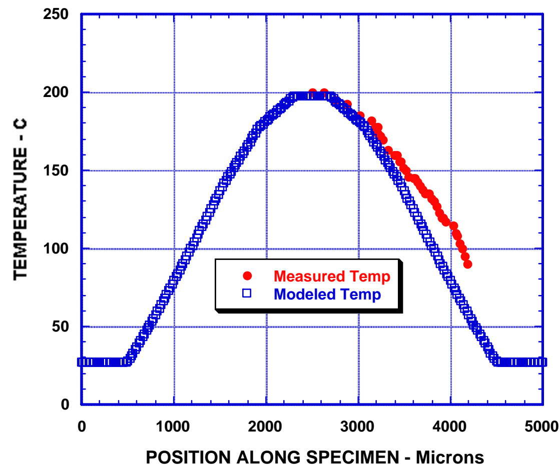

Figure 9.1 – Predicted and measured temperatures along the length of a wide specimen.

Strain is measured over a gage length of 250 µm, so the temperature variation is only a few degrees. Figure 2.5 is a photograph of the heated central region.

After the first year, Microcosm had other commitments and priorities, so the thin-film modeling was taken over by Dr. Bagdahn, who had experience with ANSYS as part of his thesis work. He explored the effect of the reflective markers on the measured strain for a polysilicon tensile specimen that is 1.5 µm thick and 50 µm wide with gold markers 10 µm wide and 0.5 µm thick. Results are presented in Figure 9.2.

The ordinate is the ratio of strain measured by the ISDG to the actual strain in the specimen; one expects that the reinforcing effect of the markers would produce a locally smaller strain. The abscissa is the spacing between the two markers. The longer the gage length the smaller the effect. The top two plots compare the strain as calculated between two points in the center of the specimen underneath each marker. One of the plots assumes the gold markers remain elastic, while the other assumes the gold to yield (the actual local stresses do exceed the yield strength of the gold). The strain in the other four plots is computed from relative displacements of points on the corners of the gold lines and in the center of the gold lines.

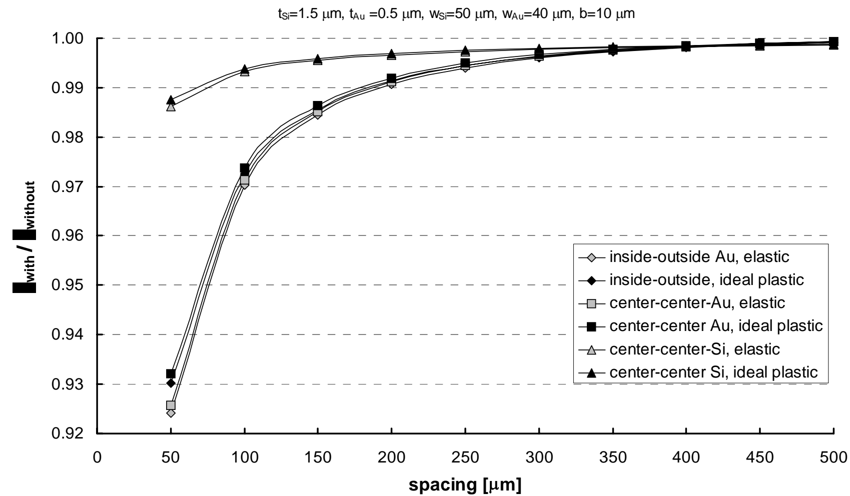

Figure 9.2 – Effect of gold markers on measured strain.

A spacing of 250 μm is normally used, and the figure shows that the computed error is 1% or less -- no matter what the assumptions of the model are. This confirms the long-held belief that the ISDG is giving accurate measurements.

10.0 – LIGA nickel stress-strain at temperature and TCE.

When the proposal was first written, Drs. Last and Garvick of the Naval Surface Warfare Center would supply LIGA Ni thick-film (~200 μm) specimens for microsample testing. Stress-strain curves and CTE data for these LIGA Ni microsamples would be obtained at temperatures between RT and 600 ^{o}C.

By the time this project ended, a considerable effort had gone into the study of LIGA Ni structures. The vast majority of LIGA structures tested in this study were fabricated at the Center for Advanced Microstructure & Devices (CAMD) at LSU in close collaboration with Jost Gottert, Kun Lian and their colleagues at CAMD [19-22]. The findings, which are described below, can be summarized as follows.

- Current LIGA processing generally results in electrodeposited nickel structures that have an attractive balance of room temperature properties,
- However, these properties have been found to be extremely sensitive to processing parameters, and thermal exposure has been shown to result in microstructural instabilities and significant property variations,

- These variations currently limit the use of LIGA structures in elevated temperature MEMS applications, e.g. such as heat exchangers, thermal actuators, micro gas turbines, power generation devices and hot embossing molds,

- Tighter control of deposition parameters and the development of novel processing routes for fabricating elevated temperature LIGA MEMS materials should be the twin goals of the future research and development of LIGA structures.

In the first year of this study, a study was completed of the room temperature microsample tensile properties of Naval Surface Warfare Center (NSWC) samples that were deposited at current densities from 3 to 50mA/cm^2 and clearly showed that the Young's modulus and yield strength both depend on the current density. Microstructural observations have confirmed the fact that decreasing the current density from 50 to 6mA/cm^2 results in a finer microstructure (smaller grain size) and a loss of out-of-plane texture. The loss of (001) texture results in an increase of the Young's modulus from 180 GPa to 207GPa, and the grain refinement led to Hall-Petch strengthening and an increase in the yield strength from 300 to 900 MPa.

LIGA-Ni samples supplied by NSWC were also used to explore the effect of annealing temperature on the microstructure and tensile properties. Stress-strain curves for samples that were annealed for 1 hour at 400, 500 and 600°C are shown in Figure 10.1 below. Specimens were unloaded and reloaded 3-4 times in each test to obtain the Young's modulus (E), and the modulus of the as-processed samples was measured to be 201GPa, which is approximately the same as for bulk Ni, 205GPa. The Young's modulus was found to be independent of the annealing temperature. By contrast, the yield strength exhibited strong temperature dependence, as it decreased dramatically with increasing annealing temperature.

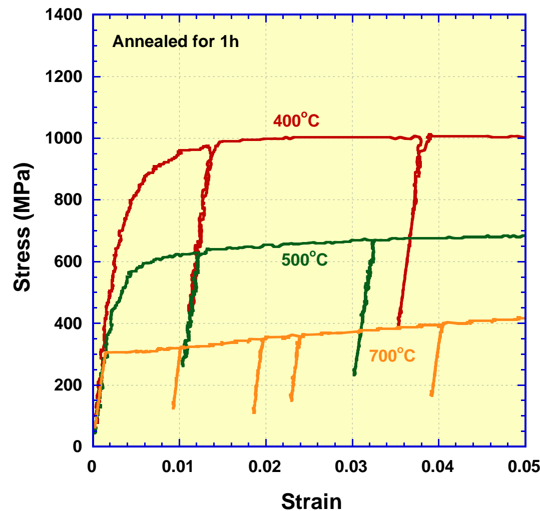

Figure 10.1 - Room temperature tensile tests of LIGA Ni samples that have been annealed for 1 hour at various temperatures.

Testing at elevated temperatures necessitated the use of wider samples, the spot size of the pyrometer is 300 μm, and the emphasis of the study was shifted to the CAMD samples. In addition to allowing for elevated temperature measurements, the CAMD samples allowed for a parametric study of the effects of processing conditions on the mechanical performance of LIGA Ni structures. Wafers were manufactured containing 118 microsamples with systematic variations in: (i) gage width (50μm to 500μm), (ii) microsample orientation (0, 45, 90°) and (iii) bath location. Room temperature tests were conducted on these specimens to see if the tensile properties are dependent on the orientation, aspect ratio (ranging from 0.6 to 5.5), and position of microsamples deposited on 4-inch wafers placed vertically in the electroplating bath. The plating conditions included a current density of 20mA/cm^2 and a bath temperature of 55°C.

No orientation dependence of Young's modulus was observed for the 400 micron wide microsamples that were tested. The measured average of E=174±15GPa is comparable with calculations based on the C_{ij}'s for single-crystalline Ni and the (001) out-of-plane texture that has been measured for this material (171~177GPa). This value is also in agreement with the values previously obtained and reported for NSWC LIGA Ni samples. The yield strength of these specimens was measured to be 366±18 MPa. There appears to be a slight variation in the yield strength with orientation, but more detailed data is needed to confirm this effect.

The yield strength of 17 microsamples having widths from 100μm to 500μm was measured to be 372MPa±17MPa. It is very important to mention that yield strength decreased to 309MPa (about 20%) when the sample's width decreases to 50μm (with an aspect ratio of ~5.5). This result implies that strength of the LIGA Ni structure having high aspect ratio in MEMS devices could be much lower than values reported in literatures where the tensile samples generally have very low aspect ratios. The average of the Young's modulus was measured to be 163±15GPa and no clear dependence of Young's modulus on aspect ratio was observed.

High temperature tensile curves are shown below in Figure 10.2. Yield strength was measured to be 323MPa, 224MPa and 134MPa at 200°C, 300 ^{o}C and 400°C, respectively. It is important to note that the yield strength at 400°C was decreased by 60% as compared with the room temperature yield strength of 372MPa±17MPa. A Cottrell-Stokes temperature-change experiment was conducted to separate the influence of temperature on the microstructure from the effect of temperature on the deformation process itself; these showed that the effect of microstructural change in this report is much more significant than expected. The implication here is that even a short period of loading at high temperature will severely degrade the performance of the material.

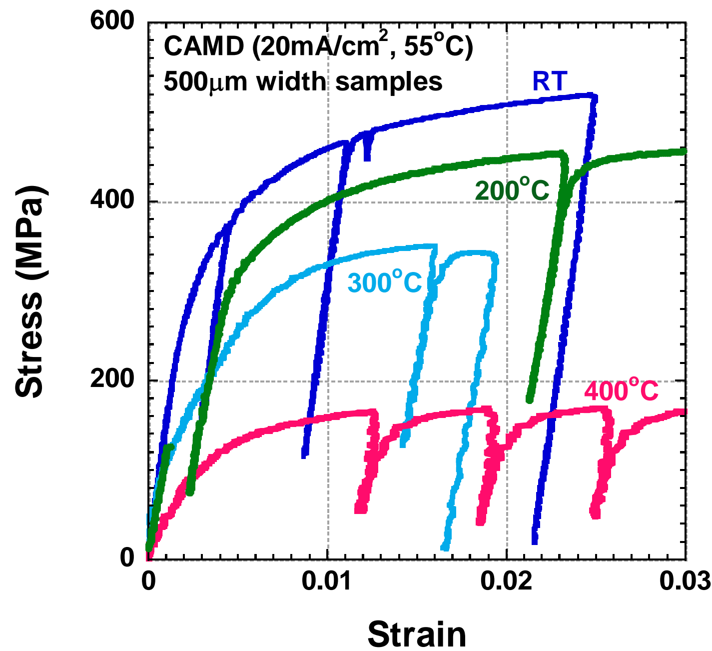

Figure 10.2 - Effect of test temperature on the properties of LIGA Ni structures.

Measurements of the coefficient of thermal expansion (CTE) were made on a CAMD LIGA nickel sample. While heating up and cooling down the sample in the creep frame at a constant stress of less than 10MPa, the strain was recorded with the ISDG. Temperature was measured by the thermocouple glued directly down to the surface of a microsample, and strain measurement was carried out for only one side in TCE measurement test instead of on both sides as usual. The strain change with temperature is shown in Figure 10.3. The TCE was measured to be slightly higher than that of pure Ni especially at the higher temperatures. The out-of-plane texture of the LIGA Ni sample is not expected to be responsible for this discrepancy; the more probably cause of this discrepancy is creep at the higher temperatures. The fact that low temperature values are close to that for bulk Ni suggests that the CTE of LIGA is the same as for bulk Ni, as expected.

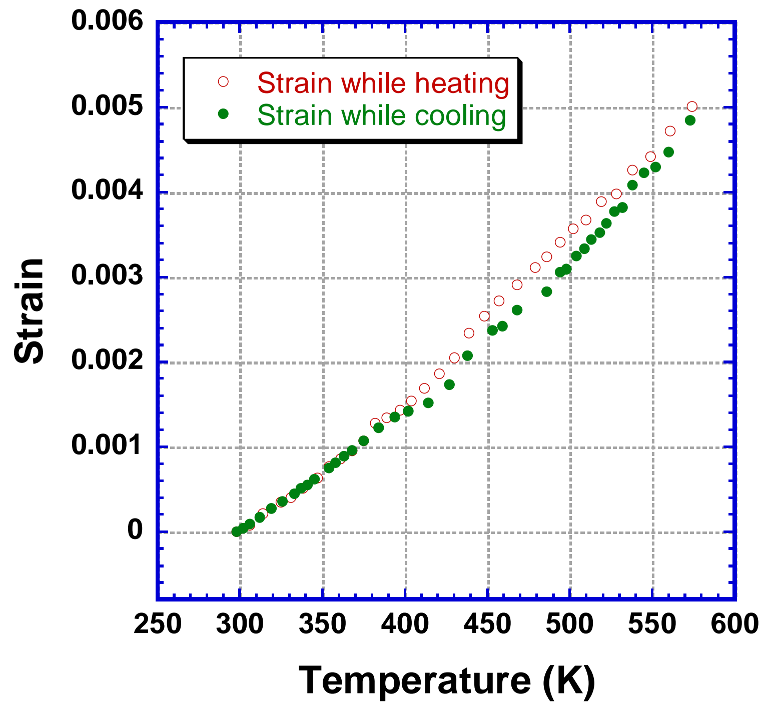

Figure 10.3 - Measurements of the CTE of LIGA Ni.

Mukherjee and colleagues have shown that electro-deposited nanocrystalline Ni exhibits superplastic behavior at intermediate temperatures, e.g. 300-400°C. The tensile elongation was measured for the CAMD LIGA Ni that was deposited at 20mA/cm^2 and had grain size of 500-1000 nm at a temperature of 400°C. The result of this exercise indicates that, while the LIGA Ni structures are not superplastic, they do show considerable ductility and toughness.

In the last year of the study, the work on LIGA Ni was extended to include the modeling, fabrication and measurement of the elastic performance of serpentine springs. Difficulties associated with processing of the serpentine springs limited the number of different materials that could be tested before the end of the project, but overall the collaboration between CAMD and JHU has been very beneficial for both parties.

Sixteen framed serpentine spring specimens have been tested, and a typical force vs. displacement curve can be seen in Figure 10.4, along with images of the springs during testing. A more detailed characterization of the dimensions was taken for these specimens. Some observations are that the topside of the specimen has a decrease in the bend width and for the same design; the dimensions vary by 1 – 2 microns. A 3-D FEM analysis shows that the spring constant is very sensitive to dimension change. During testing, after reaching the proportional

limit, the specimens were unloaded and reloaded. The spring constants increased slightly in each case due to strain hardening effects taking place at the inner bends were the stress is highest. Analysis of these experiments is ongoing.

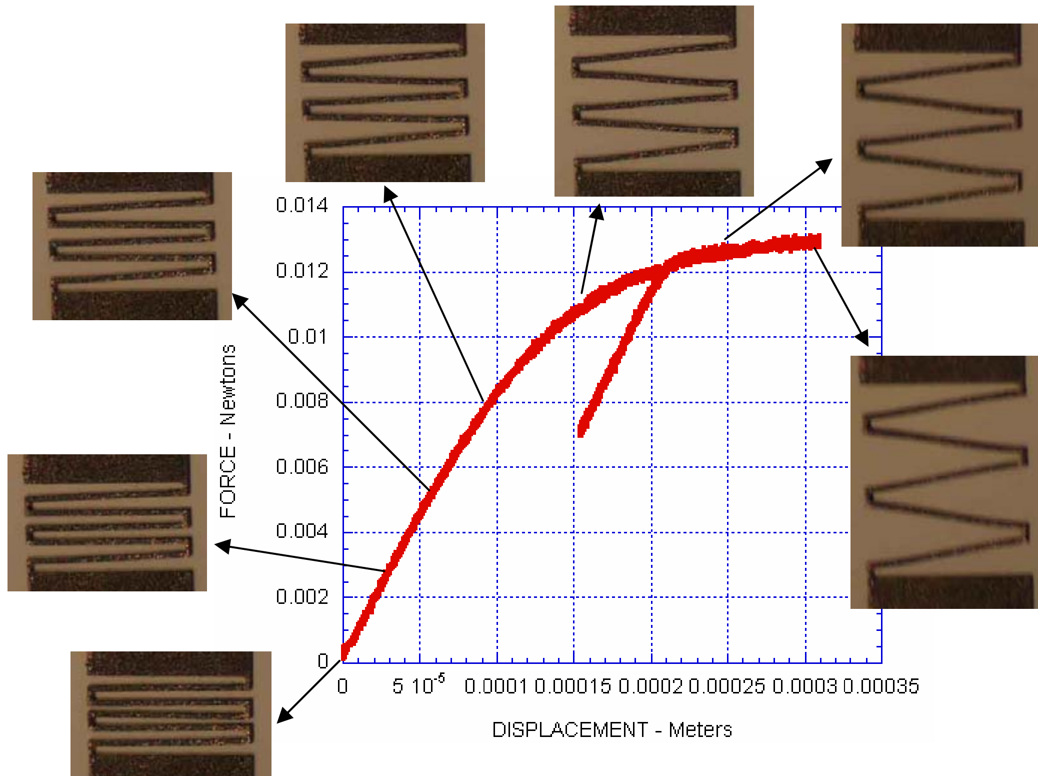

Figure 10.4 - Force vs. Displacement curve for Spring 12 along with photographs of the deformed states.

11.0 – MIT silicon carbide.

The MIT Microengine project originally proposed to use silicon carbide as the material and has been working on producing thicker material - ~40 µm or more thick – for some time. Strength and modulus are obviously important properties needed for the design, and Professor Mark Spearing has collaborated by providing wide specimens. As in the CWRU case, specimen preparation turned out to be difficult.

The process is different for this thicker material. MIT etches the mold into a silicon wafer and then sends it to a company in California that deposits silicon carbide into it via a proprietary process. The returned wafer is coated with silicon carbide on both sides. The backside must be removed so that the window can be etched into it, and the overcoat on the front side must be polished off so that the specimen is exposed. This is all quite time-consuming because silicon carbide is a very hard material. Mechanical polishing with a lapping machine was tried, but it was too damaging to the specimens; all were prepared by hand polishing.

Since silicon carbide is resistant to chemical attack, it is in principle easier to release. The first specimen dies were simply etched in KaOH to dissolve away the silicon, but the residual stresses were so high that the specimens looked like potato chips. Changes in the deposition steps reduced this in later versions. A process using a photoresist mask and xenon difluoride etchant was developed by Dr. Jackson to free the gage section. The gold strain markers had previously been deposited at APL. A specimen ready for mounting is shown in Figure 11.1. Note that the side support strips have a notch in them so they can be cut more easily.

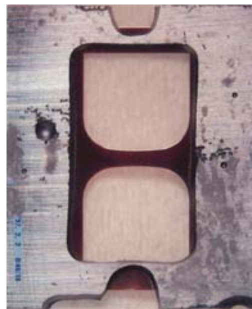

Figure 11.1 – A silicon carbide specimen from MIT; it is 30 µm thick.

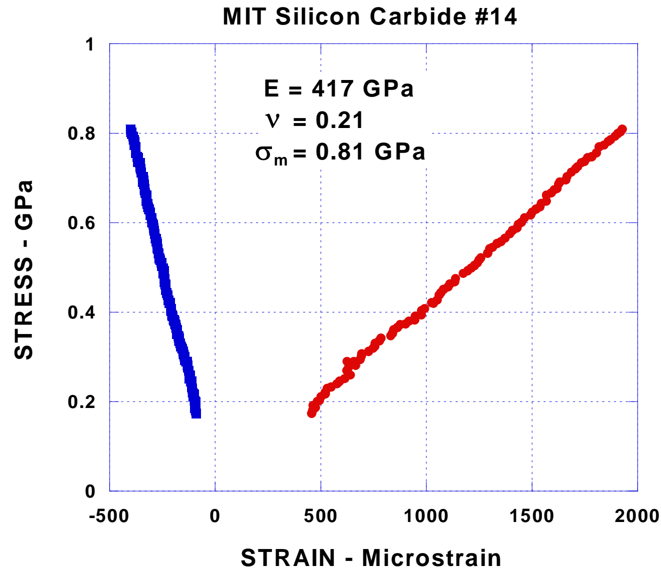

Figure 11.2 – Stress-strain curve for MIT silicon carbide.

The stress-strain curve in Figure 11.2 is similar to the ones for polysilicon and silicon nitride, but many of the specimens had defects in the markers that prohibited strain measurement. Achievement of these outstanding results is a tribute to the skill and patience of Dr. Jackson.

Batches from two different runs of MIT silicon carbide were received, and the cumulative results are presented in Table 11.1 [23].

Table 11.1 – Properties of MIT silicon carbide.

	Number of tests	Young's modulus GPa	Number of tests	Fracture strength GPa
Batch one	4	428 (395-485)	11	0.49 ± 0.20
Batch two	5	448 (423-458)	12	0.81 ± 0.23

Five measurements of Poisson's ratio were successful with an average of 0.20. The modulus is similar to the CWRU material, as one would expect. The strength results again have a large scatter and again are better for the second batch. The strengths are also low, which is a concern.

12.0 – LIGA Ni fatigue

Large specimens of CAMD LIGA Nickel were tested in a fatigue tester that is similar in concept to the one used for polysilicon, but uses a voice-coil actuator instead of a loudspeaker. The specimens were re-designed to conform to ASTM standard E466, which requires a gentle curvature to concentrate the maximum stress in the center of the specimen. Figure 12.1 shows

the shape. Tests were conducted in tension with R = 0.1 (minimum stress = 10% of maximum stress) at a frequency of 200 Hz [24-26].

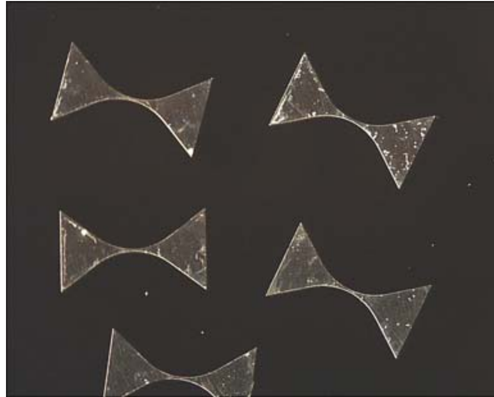

Figure 12.1 - Optical micrograph of ASTM standard E466 LIGA Ni fatigue specimens; gage width is 50 μm and specimens are 3.7 mm long.

A compilation of the results from these experiments is shown in Figure 12.2. The lines labeled 'annealed nickel' and 'hardened nickel' bound the range of fatigue values reported in the literature for bulk Ni. The triangular data points are those taken in earlier studies using microsamples designed for tensile testing, which were observed to fail at the corners where the gage meets the shoulder of the microsample. The experimental data for the new ASTM standard E466 microsamples are shown as square data points on this curve. These LIGA Ni samples show much longer fatigue lives, and the failure of these specimens all occur in the middle of the gage section, as expected. The new samples resulted in many run out tests and show an apparent fatigue limit of approximately 370 MPa.

It is encouraging to note that the E466 samples exhibit a much greater fatigue resistance than both the previous microsamples and the literature values for bulk nickel. These result indicate that the intrinsic fatigue resistance of LIGA Ni MEMS structures is excellent, but that the importance of component geometry cannot be overlooked. In this way, the current fatigue tests have highlighted the need to incorporate component geometry when assessing the fatigue resistance of a given LIGA structure.

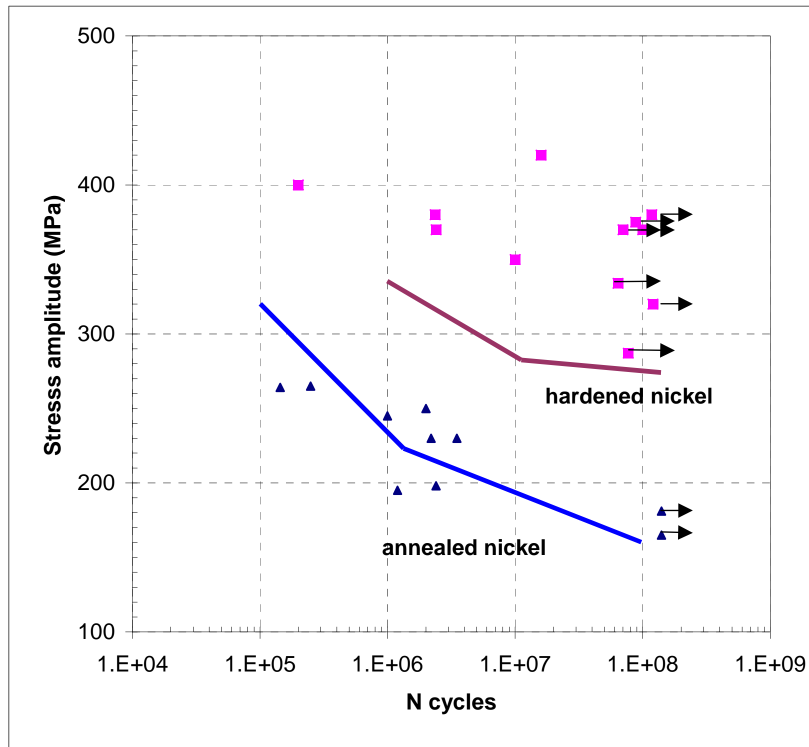

Figure 12.2 - LIGA Ni fatigue data.

13.0 – LIGA nickel Creep

The goal of this task was to characterize the creep behavior of LIGA Ni in terms of microstructural stability and thermally activated deformation processes. A number of microsamples were heated to an elevated temperature between 265°C and 400°C, loaded with a stress ranging from 100MPa to 150MPa that is lower than yield strength at that temperature, and allowed to creep slowly with time. Typical strain-time creep curves are shown below in Figure 13.1. The reduction of creep rate during "primary creep" and the attainment of a relatively constant "steady-state" creep-rate are similar to what is commonly observed during pure metal creep [24-26].

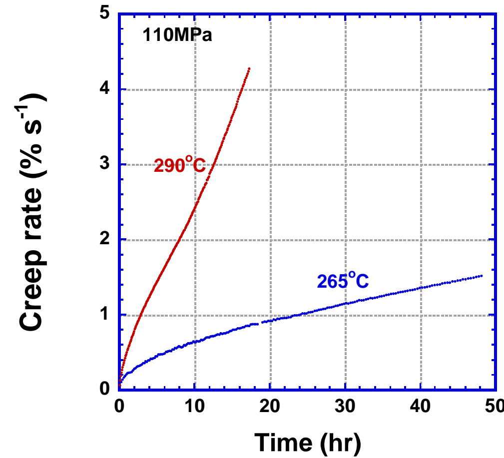

Figure 13.1 - Creep curves of LIGA Ni at relatively modest temperatures.

The measured creep rates have been normalized by the temperature dependent diffusion rates and are plotted as a function of normalized stress in Figure 13.2. The activation energy ($Q_{creep} = Q_{self\ diffusion}$ = 279 kJ/mole) and stress exponent (n = 6.5) suggest that the processes that control creep in the LIGA Ni structures are similar to those that are active in bulk polycrystalline Ni. The creep rates are, however, much higher than would be observed in bulk Ni specimens.

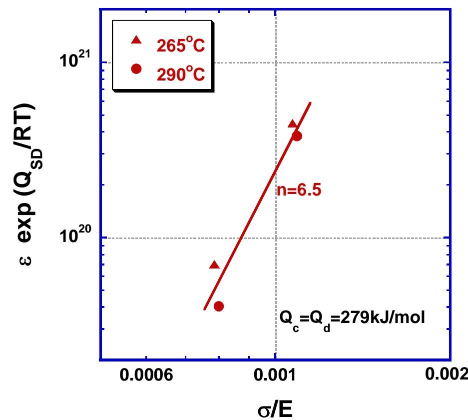

Figure 13.2 - Composite plot of the temperature and stress dependence of creep rates measured in this study.

The extremely poor creep resistance of LIGA Ni structures that was discovered in this work may be explained by microstructural instabilities and is consistent with anecdotal evidence of room temperature creep problems that have been reported by colleagues in the MEMS community. These observations suggest that the search for improved LIGA materials must be predicated on the realization that very few pure metals are used in structural engineering applications. Efforts to develop co-deposited alloys similar to high temperature Ni-base alloys will most likely be required to assure adequate creep resistance.

14.0 – Thick film microstructural studies.

Parametric studies were conducted on the effects of time and temperature on the microstructural evolution of as-deposited LIGA Ni microsamples [19]. The as-deposited microstructure is dominated by the presence of columnar grains that traverse the thickness of the microsamples and average 2-4 microns in width. Dramatic grain growth and a transition to an equiaxed grain morphology were observed in samples that were annealed for 1 hour at 800 °C. Additional cross-sectional optical micrographs, Figure 14.1, showed a transition from the as-deposited columnar microstructure to more equiaxed grains at temperatures between 400-500°C after 1 hour annealing. Extensive grain growth was observed above 500°C. The change in grain size and morphology that is evidenced in these micrographs provide a clear explanation for the decrease in strength that was measured and reported earlier.

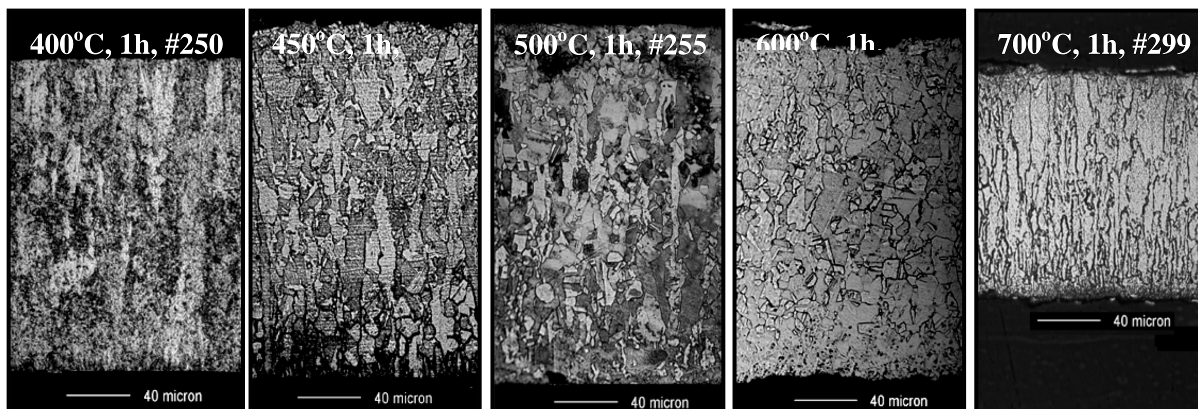

Figure 14.1 - Cross-section optical micrographs of LIGA Ni specimens that have been heat-treated to a variety of times and temperatures.

Scanning electron microscopy (SEM) observations of LIGA Ni fracture surfaces of creep and fatigue specimens were also investigated and are compared with the as-deposited microstructure in Figure 14.2. The creep rupture experiment was conducted at 400°C and 110MPa and the fatigue specimen was cycled to failure. The fatigue fracture surface resembles the as-deposited microstructure; note the trace of the initial columnar microstructure in the fracture surface. This observation suggests that intergranular fracture and grain morphology play an important role in determining the fatigue behavior. By contrast, the fracture surface of the creep rupture specimen suggests that the columnar structure has been removed during the elevated temperature creep test. This observation is consistent with the general observation that the as-deposited fine columnar microstructure is unstable. It appears that microstructural instability is the cause of the low creep strength of LIGA Ni (Task 12) and the loss of tensile strength as a result of thermal exposure (Task 9).

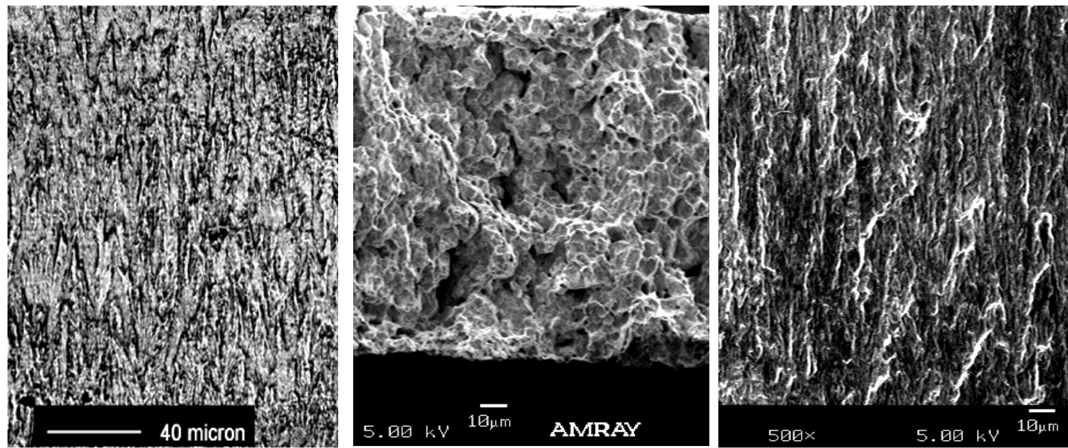

As-deposited Creep rupture surface Fatigue fractured surface

Figure 14.2 - Comparison of cross-section SEM micrographs of the fracture surfaces of LIGA Ni specimens that have been tested in fatigue and creep with the as-deposited grain structure.

15.0 – Modeling of thick films.

Originally it was felt that modelling of thick films would require more resources and follow the work performed under the modelling of thin films task. As the project progressed, however, the requirement never materialized.

A 3-D model of the large specimen had been developed by Dr. Howard Last, then of the Naval Surface Warfare Center, to study the stress distribution, and that work is published in [*H.R. Last, K. J. Hemker and R. Witt, "MEMS Material Microstructure and Elastic Property Research", Mat. Res. Soc. Symp. Proc., 605, pp. 191-196 (2000)*]. That effort, which occurred before this project started, obviated the need for further effort. Later in the program, CAMD became interested in serpentine springs, and Ms. Elmufdi conducted a thorough study, which is described under Section 10.

16.0 – Summary

New test methods were developed and new material properties measured in the course of this multi-faceted research project. Many valuable contributions to mechanical testing of MEMS materials were made. Some materials have been tested in sufficient numbers that the results may be regarded as “handbook” values, i.e. they may be used initial designs. These results were presented in the table in the beginning of this report in the Foreword section. It should be noted that the table is the first such listing for materials that were all tested in the same laboratory.

Readers seeking more in depth information can review the references provided at the end of the report or contact the authors directly.

17.0 - References

[1] Sharpe, W. N., Jr., Jackson, K., Coles, G., and LaVan, D. A., "Mechanical Properties of Different Polysilicons", *ASME Symposium on Micro-Electro-Mechanical Systems (MEMS),* Orlando, FL, MEMS-Vol.2, pp. 255-259, (November 5-10, 2000).

[2] Sharpe, W. N., Jr., Jackson, K., and Coles, G., "Young's Modulus and Fracture Strength of Three Polysilicons", *Materials Science of Microelectromechanical System (MEMS) Devices III*, MRS Proceedings Volume 657, Boston, pp. EE 5.5.1-6 (2001).

[3] Lavan, D. A., Tsuchiya, T., Coles, G., Knauss, W. G., Chasiotis, I., and Read, D., "Cross Comparison of Direct Strength Testing Techniques on Polysilicon Films", *Mechanical Properties of Structural Films, ASTM STP 1413*, West Conshocken, PA, pp. 16-27, (2001).

[4] Eby, M. A., Sharpe, W. N., Jr., and Coles, G., "Mechanical Properties of Polysilicon between 0°C and 250°C", *Proceedings of the MEMS: Mechanics and Measurement Symposium*, Society of Experimental Mechanics, Portland, pp. 16-19, (June, 2001).

[5] Sharpe, W. N., Jr., Eby, M. A., and Coles, G., "Effect of Temperature on Mechanical Properties of Polysilicon", *Proceedings Transducers '01,* Munich, pp. 1366-1369, (June, 2001).

[6] Sharpe, W. N., Jr., Jackson, K. M., Hemker, K. J., and Xie, Z., "Effect of Specimen Size on Young's Modulus and Fracture Strength of Polysilicon", *Journal of Microelectromechanical Systems*, Vol.10, No. 3, pp. 317-326, (September 2001).

[7] Bagdahn, J., Schischka, J., Petzold, M., and Sharpe, W. N., Jr., "Fracture Toughness and Fatigue Investigations of Polycrystalline Silicon", *Reliability, Testing, and Characterization of MEMS/M0EMS,* SPIE Vol. 4558, San Francisco, pp. 159-168, (October, 2001).

[8] Bagdahn, J. and Sharpe, W. N., Jr., "Fracture Strength of Polysilicon at Stress Concentrations", *Materials Science of Microelectromechanical System (MEMS) Devices IV*, MRS Proceedings Volume 687, Boston, pp. 285-290, (2002).

[9] J. Bagdahn, W. N. Sharpe, Jr. and O. Jadaan, Fracture strength of polysilicon at stress concentrations, accepted for publication in JMEMS, February 2003.

[10] Jackson, K. M., Edwards, R. L., Dirras, G. F., and Sharpe, W. N., Jr., "Mechanical Properties of Thin Film Silicon Carbide", *Materials Science of Microelectromechanical System (MEMS) Devices IV*, MRS Proceedings Volume 687, Boston, pp. 217-222, (2002).

[11] Jackson, K. M., Dirras, G. F., Edwards, R. L., and Sharpe, W. N., Jr., "Mechanical Properties of 3C Thin-Film Silicon Carbide", *Proceedings of the 2002 SEM Annual Conference*, Milwaukee, pp. 99-104, (2002).

[12] Coles, G., Sharpe, W. N., Jr., and Edwards, R. L., "Mechanical Properties of Silicon Nitride", *Proceedings of the MEMS: Mechanics and Measurement Symposium*, Society of Experimental Mechanics, Portland, pp. 1-4, (June, 2001).

[13] Brown, S., Edwards, R. L., Panth, R., Bergstrom, J., Coles, G., and Sharpe, W. N., Jr., "A Comparison between Tensile and Bulge Test Methods for Thin Films", *MRS Fall 2001,* Boston, (November, 2001), in press.

[14] Edwards, R. L., Coles, G., and Sharpe, W. N., Jr., "Comparison of Tensile and Bulge Tests for Thin-Film Silicon Nitride", *Journal of Materials and Mechanics*, in press for 2003.

[15] J. Bagdahn, K. Jackson and W. N. Sharpe, Jr., Tensile strength of multilayer metal-glass CMOS structures, Eurosensors 2002, Prague, September 15-18.

[16] Sharpe, W. N., Jr. and Bagdahn, J., "Fatigue of Materials used in Microelectromechanical Systems (MEMS)", *FATIGUE 2002 – Proceedings of the Eighth International Fatigue Congress,* Stockholm, pp. 2197-2212, (2002).

[17] J. Bagdahn and W. N. Sharpe, Jr., Reliability of polycrystalline silicon under long-term cyclic loading, *J. of Sensors and Actuators*, in press (2003).

[18] H. R. Last, K. J. Hemker, and R. Witt, "MEMS Material Microstructure and Elastic Properties", Materials Research Society Symposium Volume 605, pp. 191-196, (2000).

[19] H. S. Cho, W. G. Babcock, H. Last and K. J. Hemker, "Annealing effects on the microstructure and mechanical properties of LIGA nickel for MEMS", *Mat. Res. Soc. Symp. Proc.*,**657**, pp EE5.23.1-6, (2001).

[20] K.J. Hemker and H.R. Last, "Microsample Tensile Testing of LIGA Ni for MEMS Applications", *Mater. Sci. and Eng. A*, 319-321 (2001) 882-886.

[21] H. S. Cho, G. Dirras, W. G. Babcock, H. Last and K. J. Hemker, "Tensile Properties of LIGA Ni Structures for a Fusing/Safety and Arming Device**",** *J. Microsystem Technologies,* in press, (2003).

[22] H.S. Cho, K.J. Hemker, K. Lian, J. Goettert and G. Dirras, "Measured Mechanical Properties of LIGA Ni Structures", *J. of Sensors and Actuators*, in press (2003).

[23] Jackson, K., M., "The Mechanical Properties of 3C Thin-Film Silicon Carbide", Ph.D. Thesis, Johns Hopkins University, (2002).

[24] H.S. Cho, K.J. Hemker, K. Lian and J. Goettert, "Tensile, Fatigue and Creep Properties of LIGA Ni Structures", MEMS 2002 Technical Digest, 15th IEEE Int. Conf. On MEMS, Las Vegas NV, 439-442, (2002).

[25] H.S. Cho, K.J. Hemker, K.Lian, J. Goettert and G. Dirras, "Tensile, Creep and Fatigue Properties of LIGA Nickel Structures", *J. of Sensors and Actuators*, in press (2003).

[26] K. J. Hemker, H. S. Cho, Y. Desta, K. Lian and J. Goettert, "Tensile, Creep and Fatigue Testing of LIGA Ni-Micro-samples", *J. Microsystem Technologies*, in press (2003).

18.0 - Overview and Review Publications

Sharpe, W. N., Jr. "Tensile Testing of MEMS Materials", *3rd International Conference and Poster Exhibition – MicroMat 2000,* Invited Presentation, abstract only, pg. 351, (2000).

Sharpe, W. N., Jr. and K. Jackson, "Tensile Testing of MEMS Materials", *Proceedings of the Microscale Systems: Mechanics and Measurements Symposium,* Society for Experimental Mechanics, Invited Presentation, pp. ix-xiv, (2000).

Sharpe, W. N., Jr., and Bagdahn, J., "Fatigue of Polysilicon – A Review", *2001 Mechanics and Materials Summer Conference,* San Diego, Abstract only, (June, 2001).

Sharpe, W. N., Jr., "Measurement of the Mechanical Properties of MEMS Materials", *6th National Congress of Mechanics*, Thessaloniki, Greece, Abstract only, (July, 2001).

Sharpe, W. N., Jr., Jackson, K., Coles, G., Eby, M. A., and Edwards, R. L., "Tensile Tests of Various Thin Films", *Mechanical Properties of Structural Thin Films,* ASTM STP 1413, American Society of Testing and Materials, Orlando, pp. 229-247, (2001).

Sharpe, W. N., Jr., "Mechanical Testing of Free-Standing Thin Films", *Materials Science of Microelectromechanical System (MEMS) Devices IV*, MRS Proceedings Volume 687, Boston, pp. 293-304, (2002).

Sharpe, W. N., Jr., Bagdahn, J., Jackson, K., and Coles, G., "Tensile Testing of MEMS Materials – Recent Progress", *Symposium on the Mechanical Properties of MEMS Structures,* Kluwer Academic Press, in press, (2003).

Sharpe completed a chapter entitled "Mechanical Properties of MEMS Materials" to appear in the CRC publication, The MEMS Handbook, CRC Press, pp. 3-1 to 3-33, (2001). This chapter with 161 references was distributed as a report to researchers with interest in material properties.

W. N. Sharpe, Jr. and J. Bagdahn, Fatigue testing of polysilicon – A review, Journal of Materials and Mechanics, in press for 2003.

W. N. Sharpe, Jr., "Tensile Testing at the Micrometer Scale (Opportunities in Experimental Mechanics)", EXPERIMENTAL MECHANICS, in press for 2003.

19.0 - Presentations

Information was disseminated numerous presentations at conferences and universities. These are listed here in more-or-less chronological form to indicate the level of effort. Many of the conference presentations were published as listed earlier.

Sharpe participated in a NSF-sponsored symposium on nanotechnology in Palo Alto October 6-8, 1999 and gave a talk entitled "Status of Mechanical Properties of MEMS Materials" at the DARPA/NSF/ONR symposium on RF MEMS in Crystal City December 1-2, 1999.

Hemker presented a talk entitled, "Effect of As-processed and Annealed Microstructures on the Mechanical Properties of LIGA Ni MEMS" at the Fall Materials Research Society (MRS) meeting in Boston MA November 29-November 3, 1999.

Sharpe presented "Tensile Testing of MEMS Materials" at MicroMat 2000 in Berlin, Germany, April 17-19, 2000. W. N. Sharpe, Jr., and K. Jackson, "Tensile Testing of MEMS Materials," Microscale Systems: Mechanics and Measurements Symposium, 2000, Society for Experimental Mechanics, pp. ix - xiv, 2000; presented at the meeting in June 2000. Sharpe presented seminar on the topic at the University of Nebraska in September, 2000. Sharpe, W. N., Jr., Jackson, K., Coles, G., and LaVan, D. A., "Mechanical Properties of Different Polysilicons", ASME Symposium on Micro-Electro-Mechanical Systems (MEMS), Orlando, FL, MEMS-Vol.2, pp. 255-259, (November 5-10, 2000); Poster presentation.

Hemker and Last, “Microsample Tensile Testing of LIGA Ni for MEMS Applications”, presented at the International Conference on the Strength of Metals and Alloys (ICSMA) in Asilomar CA, August 2000. Hemker presented a seminar entitled, “Identifying structure-property relations in materials for MEMS applications”, at the Center for Advanced Microstructures and Devices, Louisiana State University, Baton Rouge, LA, October 2000.

Sharpe presented a seminar at Cornell University September 7, 2001 and made presentations at the American Vacuum Society, San Francisco, October, 2001 and the International Semiconductor Device Research Society, Georgetown, December, 2001. Sharpe, W. N., Jr., Bagdahn, J., Jackson, K., and Coles, G., “Tensile Testing of MEMS Materials – Recent Progress”, ASME Symposium on the Mechanical Properties of MEMS Structures, 9 pages and presentation, (November, 2001).

Hemker presented a seminar on “Microstructure of MEMS Materials” at Berkeley in February, 2001.
H. S. Cho, G. Dirras, W. G. Babcock, H. Last and K. J. Hemker, “Tensile Properties of LIGA Ni Structures for a Fusing/Safety and Arming Device”, paper presented along with two posters -- K. J. Hemker, H. S. Cho, Y. Desta, K. Lian and J. Goettert, “Tensile, Creep and Fatigue Testing of LIGA-Ni Microsamples” T. Fritz, H. Cho, K.J. Hemker, W. Mokwa and U. Schnakenberg, “Characterization of Electroplated Nickel” at the Fourth International Workshop on High-Aspect-Ratio Micro-Structure Technology (HARMST) in Baden-Baden, Germany, June 17-19, 2001. Kevin Hemker also gave two invited seminars that included MEMS work supported by this grant: Institut Galilée, Université of Paris XIII, Villetaneuse, France, June 2001, “Gulliverian Studies of Structural Materials” and Laboratoire Electronique de Microscopie, CNRS-ONERA, Chatillon, France, July 2001;“Structure-property relations in MEMS materials and Thermal Barrier Coatings”. “Elevated Temperature Tensile, Creep and Long-term Fatigue Behavior of LIGA Ni MEMS Structures”, H.S. Cho, Y. Desta, K. Lian, J. Goettert and K.J. Hemker at the 2001 MRS Fall Meeting, Boston MA, November 2001.

Sharpe presented a seminar at the University of Wisconsin and made a presentation at the Washington DC area MEMS Alliance in April, 2002. Sharpe gave the Murray Medal Lecture at the Society for Experimental Mechanics meeting in Milwaukee in June, 2002; the title being “TENSILE TESTING AT THE MICROMETER SCALE (Opportunities in Experimental Mechanics)”. Sharpe presented an invited overview lecture, “Fatigue of Materials used in Microelectromechanical Systems (MEMS)” at FATIGUE 2002, the Eighth Tri-Annual International Conference on Fatigue. He also presented “Static and Cyclic Fatigue of Polysilicon”, on behalf of Dr. Bagdahn who could not attend. Sharpe organized a keynote session entitled “Microelectromechanical Systems” at the 14th U.S. National Congress of Theoretical and Applied Mechanics, Blacksburg VA, June 2002. The objective was to present research topics in solid and fluid mechanics as well as materials to the attendees. “The Read Dally Tensile Specimen”, Sharpe, 14th U.S. National Congress of Theoretical and Applied Mechanics, Blacksburg VA, June 2002. J. Bagdahn, K. Jackson and W. N. Sharpe, Jr., Tensile strength of multilayer metal-glass CMOS structures, Eurosensors 2002, Prague, September 15-18, 2002.

Hemker presented "Gulliverian Studies of Thermal Barrier Coatings and MEMS Materials" at the Dept. of Materials Science and Engineering Seminar, Lehigh University, Bethlehem, PA, March 2002. "Tensile and Fatigue Properties of LIGA Ni Structures", Elmufdi, Cionea, Hemker. (invited) at DARPA CAMD MEMS Review, Dallas TX, May 2002. "The Mechanical Behavior of LIGA Ni Structures for MEMS Applications", Hemker (invited), 14th U.S. National Congress of Theoretical and Applied Mechanics, Blacksburg VA, June 2002. Microsample tensile and fatigue testing of LIGA Ni MEMS Materials, by C. Cionea and K.J. Hemker, TMS Fall Meeting in Columbus Ohio, Oct. 7, 2002. Characterizing the Bechanical Behavior of MEMS Serpentine Springs, by C. Elmufdi and K.J. Hemker, TMS Fall Meeting in Columbus Ohio, Oct. 7, 2002.

20.0 - Personnel and Collaborators

Personnel

Sharpe, Hemker, and Edwards.
George Coles, Research Assistant in the Mechanical Engineering Department, on a full-time basis during the course of the effort.
Kamili Jackson, who conducted the silicon carbide tests and received her Ph.D.
Matthew Eby, ME undergraduate receiving B. S. in 2000.
David Sampson, ME undergraduate receiving B. S. in 2001.
Dr. Guy Dirras, Visiting Professor from France.
H. S. Cho, Postdoctoral Fellow from South Korea.
Ryan Austin, ME undergraduate to receive B. S. in 2003.
Matt Hayden, ME graduate student receiving M. S. in 2001.
Dr. Joerg Bagdahn, Postdoctoral Fellow from Germany.
Mr Cionea and Ms. Elmufdi, graduate students.
Dr. Mingwei Chen, Postdoctoral Fellow from China.

Collaborators

David Koester at Cronos, now J. D. Uniphase
David LaVan and Tom Bucheit at Sandia-Albuquerque
Carl Freidhoff at Northrup Grumman
Steve Bart at Microcosm, Inc.
Chris Zorman and Hal Kahn at Case Western Reserve University
Osama Jadann at University of Wisconsin – Platteville
Alma Wickenden at Army Research Laboratory
Stuart Brown at Exponent, Inc.
Roger Howe at Berkeley Sensor and Actuator Center
Gary Fedder at Carnegie Mellon
Noel Nemeth at NASA-Glenn

Jost Gottert at CAMD-LSU
Mark Spearing at MIT
Howard Last at Naval Surface Warfare Center